



Flexible Heat and Power, connecting heat and power networks by harnessing the complexity in distributed thermal flexibility

## **D4.5 Summary and valuation results**

Version number: 1.0

Dissemination Level: PU

Lead Partner: NODA

Due date: 31/10/2019

Type of deliverable: Report

Status: Final

Copyright © 2019 FHP Project



This project has received funding from the European Union's Horizon 2020 research and innovation programme under grant agreement No 731231.

### Published in the framework of:

**FHP<sup>1</sup>** Flexible Heat and Power, connecting heat and power networks by harnessing the complexity in distributed thermal flexibility

FHP website: [www.fhp-h2020.eu](http://www.fhp-h2020.eu)

### Authors:

Borgqvist, M. (NODA)  
Brage, J. (NODA)  
Fernandez Dominguez, M. (TECNALIA)  
Tellado Laraudogoitia, B. (TECNALIA)  
Geysen, D. (VITO)  
Suryanarayana, G. (VITO)  
Wiet Mazajrac (Ecovat)  
Lindahl, M. (RISE)  
Steen, M. (KEAB)

---

### <sup>1</sup> Disclaimer:

The content of this report does not reflect the official opinion of the European Union. Responsibility for the information and views expressed in the therein lies entirely with the author(s).

## Executive summary

The key goal – and challenge – of the pilot validation was to assess the possibility and barriers of retrofit solutions using the available P2H infrastructure (incl. off-the-shelf heat pumps that are installed), without introducing additional infrastructure that might be perceived as being too intrusive. Specifically, we wanted to evaluate the creation of dynamic thermal models purely based on measurement data (hence no model creation by a human expert), and the provision of curtailment mitigation services with legacy off-the-shelf heat pumps that are indirectly controlled using an outdoor sensor override control paradigm.

This was done through two pilot sites. The pilot in Uden, the Netherlands, was focused on the capabilities of a large 'central' P2H solution: the ECOVAT solution. For further details on the pilot validation phases and activities, see D4.3. The pilot in Karlshamn, Sweden, was focused on a distributed P2H solution – heat pumps in industrial and residential buildings in Karlshamn. For further details, on the Swedish pilot validation phases and activities, see D4.4.

These pilot activities were planned to run from October 2018 till end of April 2019. As it quickly turned out that the challenges specifically for the Swedish pilot (non-intrusive retrofit solution, expert-free dynamic thermal modelling, indirect control of heat pumps through outdoor temperature sensor override), it was decided to put priority on the validation activities for the Swedish pilot until April 2019 to not miss the heating season. The qualitative validation activities for the Dutch pilot – where there was no dependency on the heating season – were therefore postponed and once started have been continuing until October 2019. The Ecovatt pilot installation in Uden is still active, and further ongoing experiments are planned and will continue beyond the end of the FHP project. Also the owners of Premise 2.2 in Karlshamn have expressed interest in continued active control of their heatpump, and follow-up activities are being planned by NODA and KEAB.

Overall, the measurement driven dynamic thermal model creation proved to be good enough for the intended curtailment mitigation services with legacy off-the-shelf heat pumps. Specific envisaged future improvements relate to fitting multiple models for different contexts (e.g. season, ...), and enriching the available data with heat flow measurements (assuming the required infrastructure for this will become more affordable in future). Regarding the indirect control approach, there is clearly potential in further improving the heatpump signature model creation from measurements (including perturbations to get a richer training set), though this only adds value for heat pumps whose internal controller is intrinsically flexible enough. With the legacy heat pumps that were installed in the pilot buildings, and their limitations, it would be impossible to offer profile following services like balancing, though curtailment mitigation requiring less deterministic responses are judged to be possible. The lab experiments in WP2 have shown that there is a huge difference among different heatpump brands and models, and it is judged that with properly



selected heat pumps, combined with a good heatpump signature model, (close to) profile following services can be offered using the indirect control approach (depending on what level of accuracy is demanded). Hence there would be a need for a heatpump qualification and characterization service to select a fit-for-purpose heatpump. Ideally though, in future, the in WP2 proposed direct control paradigm could be employed, and related discussions and engagements with heatpump manufacturers and standardization organizations will be pursued. This direct control paradigm is seen as an essential feature that enables deterministic heatpump control which is needed for offering high value profile following services within set comfort boundaries.

This deliverable as well proposes and calculated an impact assessment KPI with respect to leveraging the active control of P2H conversions to mitigate RES-E curtailment.



## Table of content

Executive summary .....	3
Table of content .....	5
Abbreviations.....	10
1 Introduction .....	11
2 Dutch Pilot - Ecovat.....	12
2.1 Model accuracy .....	12
2.1.1 The Ecovat dynamic thermal model .....	12
2.1.2 The Heat pump signature model for indirect control .....	15
2.2 Demand profile following capabilities .....	21
2.2.1 Test profile .....	21
2.2.2 Analysis .....	22
3 Swedish Pilot, VITO building agent services .....	25
3.1 Model Accuracy .....	25
3.1.1 The heatpump signature model for indirect control .....	25
3.1.2 The building dynamic thermal model.....	26
3.1.3 Quality of exogenous parameters .....	31
3.1.4 Quality of sensor data .....	32
3.2 Demand profile following capabilities .....	33
3.2.1 Background .....	33
3.2.2 Analysis .....	34
3.2.3 Summary of learnings from VITO integrations tests. ....	45
4 Swedish Pilot, TECNALIA building agent services .....	48
4.1 Model accuracy .....	48
4.1.1 Background .....	48
4.1.2 Analysis .....	48
4.2 Demand profile following capabilities .....	55
4.2.1 Background .....	55
4.2.2 Analysis .....	55
5 Impact Analysis by extrapolation of results.....	59
5.1 Scenario .....	59
5.1.1 Flexibility provided by buildings.....	60
5.1.2 Flexibility provided by ECOVATs .....	61



5.2	Data .....	61
5.3	Results .....	64
6	Conclusion and next steps .....	71
7	References .....	74



**List of tables**

Table 1: The training and validation errors for the model that learns the relation between the power consumption and supply temperature .....	19
Table 2: Error quantification for a 4hr timestep curtailment mitigation service. ..	24
Table 3: RMSE of building model training .....	31
Table 4: Overview of selected tests in Swedish pilot .....	33
Table 5: Performance indicators of the individual buildings for the No_Flex test. ..	35
Table 6: Pearson correlation and MAPE values for indoor temperature forecasting in both premises. ....	51
Table 7: Baseline, consumption and relative billing impact during the testing period. Values for the days in which the minimum and maximum baseline was computed are shown. ....	53
Table 8: Summary of result for days in which maximum and minimum baselines were computed. ....	54
Table 9: Pearson correlation and SMAPE for the delivered consumption profile and the real one.....	57
Table 10: ECOVAT market share in terms of standard deviations of the intraday market.....	61
Table 11: Comparison of distributions: SD(Before) / SD(After) – 1. ....	69

**List of figures**

Figure 1: Charge test: measured vs. modeled temperatures .....	12
Figure 2: Discharge test: measured vs. modeled temperatures .....	13
Figure 3: Combined test: measured vs. modeled temperatures .....	14
Figure 1: Ramping up test: the response of the electric power consumption and supply temperature to changes in the outdoor temperature override. ....	16
Figure 2: Ramping up test: scatter plot of supply temperature vs outdoor temperature (the dark grey line superimposed to reflect the input heat curve)...	16
Figure 3: Ramping down test: the response of the electric power consumption and supply temperature to changes in the outdoor temperature override. ....	16
Figure 4: Ramping down test: scatter plot of supply temperature vs outdoor temperature (the dark grey line superimposed to reflect the input heat curve)...	17
Figure 5: Mixed test: the response of the electric power consumption and supply temperature to changes in the outdoor temperature override. ....	17
Figure 6: Mixed test: scatter plot of supply temperature Vs outdoor temperature (the dark grey line superimposed to reflect the input heat curve). ....	18
Figure 7: The data used to train the heat pump model, and the resulting fitted values.....	20
Figure 8: Validation of the model for a part of data in the ramping up test. ....	20
Figure 9: Validation of the model in ramping down test. ....	20
Figure 10: Validation on the data from the mixed test.....	21
Figure 11: A zoomed in version of the ramp up test, to focus on the delays in response of the supply temperature to change in outdoor temperature. ....	21



Figure 12: Test profile for the heat pump. .... 22

Figure 13: The response of the electric power consumption and supply temperature to the control signal..... 23

Figure 14: Planned consumption (blue) vs actual consumption(orange)..... 23

Figure 15: Planned supply temperature(blue) vs actual supply temperature(orange). .... 24

Figure 16: Heatpump signature for P1.2 (West), computed over three months of hourly data..... 25

Figure 17: Input data for P2.1 (residential building)..... 26

Figure 18: Results of auto-validation fitting for P2.1 (residential building). .... 27

Figure 19: Fitted results from P1.2 (East) (industrial building). .... 29

Figure 20: P1.2 (East) cross validation results (industrial building). .... 30

Figure 21: Fitted P2.3 results..... 31

Figure 22: Distribution of the accuracy of the forecasted outdoor temperatures in Karlshamn, Sweden, with mean 0.4 °C and standard deviation 1.5 °C ..... 32

Figure 23: Comparison building control signal and actual power consumption of the buildings in test No\_Flex (4-hour average). .... 36

Figure 24: Comparison building control signal and actual power consumption of P2.1 (5-min average)..... 37

Figure 25: Average indoor temperature and comfort boundaries. .... 37

Figure 26: Comparison building control signal and actual power consumption of the buildings in test Flex\_1 (4-hour average). .... 38

Figure 27: Comparison building control signal and actual power consumption of the buildings in test Flex\_2 (4-hour average). .... 39

Figure 28: Comparison of the planned cluster consumption profile and the actual aggregated measured consumption of the cluster in test Flex\_2..... 39

Figure 29: Summary of P1.2 (E) data in Flex\_2 test. .... 40

Figure 30: Summary of P2.1 data in Flex\_2 test..... 40

Figure 31: Summary of P2.3 data in Flex\_2 test..... 41

Figure 32: Comparison building control signal and actual power consumption of the buildings in test Flex\_3 (4-hour average). .... 42

Figure 33: Comparison of the planned cluster consumption profile and the actual aggregated measured consumption of the cluster in test Flex\_3..... 42

Figure 34: Summary of P1.2 (E) data in Flex\_3 test. .... 43

Figure 35: Summary of P2.1 data in Flex\_3 test..... 43

Figure 36: Summary of P2.3 data in Flex\_3 test..... 44

Figure 37: Building control signal and temperature offset Premise 2.1 in Flex\_3 test. .... 44

Figure 38: Day ahead consumption and indoor temperature forecast flow. .... 48

Figure 39: Measured indoor temperatures in the P2.1 apartments. .... 49

Figure 40: P2.1 indoor temperatures (average)..... 49

Figure 41: Measured indoor temperature in the P2.3 apartments. .... 50

Figure 42: P2.3 indoor temperatures (average)..... 50

Figure 43: Incentives/penalties profiles..... 52



Figure 44: Building control signal response to incentives for P2.1 (left) and P2.3 (right) compared to the baseline consumption. .... 52

Figure 45: P2.1 energy profiling. .... 56

Figure 46: P2.3 energy profiling. .... 56

Figure 47: Forecasted and measured outdoor temperature. .... 58

Figure 48: Distribution of  $\Delta_{max}P/P_{mean}$  based on 70 buildings in Karlshamn, Sweden..... 61

Figure 49: Belgium: Intermittent RES-E [MW] Day Ahead. .... 62

Figure 50: Belgium: Intermittent RES-E [MW] Intraday - Day Ahead. .... 63

Figure 51: Belgium: Intermittent RES-E [MW] Current - Intraday. .... 63

Figure 52: Belgium: Solar [MW] Current (Before, After  $\pm 1$  SD). .... 64

Figure 53: Belgium: Wind Offshore [MW] Current (Before, After  $\pm 1$  SD). .... 65

Figure 54: Belgium: Wind Onshore [MW] Current (Before, After  $\pm 1$  SD)..... 65

Figure 55: Belgium: Total [MW] Current (Before, After  $\pm 1$  SD). .... 66

Figure 56: Belgium: Solar [MW] Current KDE (Before, After  $\pm n$  SD). .... 67

Figure 57: Belgium: Wind Offshore [MW] Current KDE (Before, After  $\pm n$  SD). ... 67

Figure 58: Belgium: Wind Onshore [MW] Current KDE (Before, After  $\pm n$  SD)..... 68

Figure 59: Belgium: Total [MW] Current KDE (Before, After  $\pm n$  SD). .... 68

Figure 60 Belgium: Total [MW] Current CDF (Before, After  $\pm$  SD)..... 70



## Abbreviations

Short form	Long form
BRP	Balancing Responsible Party
CDF	Cumulative Distribution Function
COP	Coefficient of Performance
DA	Day-Ahead
DAM	Day-Ahead Market
DCM	Dynamic Coalition Manager (extension/specialisation of Aggregator)
DER	Distributed Energy Resource
DHW	Domestic Hot Water
DSO	Distribution System Operator
EV	Electrical Vehicle
ID	Intraday
KDE	Kernel Density Estimate
LDC	Load Distribution Curve
RES	Renewable Energy Source
RES-E	Renewable Energy Source, Electricity
RMSE	Root Mean Square Deviation
sMAPE	symmetric Mean Absolute Percentage Error
ToU	Time of Use

## 1 Introduction

The FHP project<sup>2</sup> – *Flexible Heat and Power: connecting Heat and Power networks by harnessing the complexity in distributed thermal flexibility* – was submitted under the call *LCE-01-2016-2017: Next generation innovative technologies enabling smart grids, storage and energy system integration with increasing share of renewables: distribution network*, more specifically under the *Synergies between Energy Networks* area.

This deliverable summarizes the validation results of the two pilots in relation to the goals of the project and the technology that was developed.

- The pilot in Uden, the Netherlands, was focused on the capabilities of a large concentrated P2H solution - the ECOVAT solution - and its connection to the electrical grid, and its interaction with the DSO.
- The pilot in Karlshamn, Sweden, was focused on distributed P2H solutions and the challenges related to expert-free modelling of the available flexibility.

The two pilots demonstrated how thermal flexibility – provided by P2H conversions in combination with thermal storage - can be used to avoid curtailment of intermittent RES-E or, what amounts to the same thing, increase the effective distribution capacity of the electrical grid (e.g. distributing more energy over the present infrastructure). To this purpose, a DCM-centric multi-agent platform has been deployed and used, that is implementing a Flex Trading interaction scheme that goes beyond traditional Demand Response approached by the fact that the flexible assets themselves pro-actively determine and communicate their own (optimal) consumption plans as well as the available flexibility.

The key goal – and challenge – of the pilot validation was to propose – and assess the possibility and barriers of – retrofit solutions using the available P2H infrastructure (incl. off-the-shelf heat pumps that are installed), without introducing additional infrastructure that might be perceived as being too intrusive. Specifically, we wanted to evaluate the creation of dynamic thermal models purely based on measurement data (hence no model creation by a human expert), and the provision of curtailment mitigation services with legacy off-the-shelf heat pumps that are indirectly controlled using an outdoor sensor override control paradigm.

---

<sup>2</sup>See <http://www.fhp-h2020.eu/> and [http://cordis.europa.eu/programme/rcn/700614\\_en.html](http://cordis.europa.eu/programme/rcn/700614_en.html)

## 2 Dutch Pilot - Ecovat

For this pilot, the source of flexibility came from the Ecovat built in the Netherlands. The pilot description and the setup has been explained in the earlier deliverables. Here, we focus on the test results.

### 2.1 Model accuracy

As in the case of buildings, the flexibility in the thermal mass of the Ecovat is accessed through the heat pump. To be able to utilize the available flexibility optimally, we need a thermal model of the Ecovat thermal storage vessel, as well as a heatpump signature model for the P2H conversion

#### 2.1.1 The Ecovat dynamic thermal model

The Ecovat dynamic thermal model is based on the method described in "De Ridder, Fjo, and Mathias Coomans. "Grey-box model and identification procedure for domestic thermal storage vessels." Applied Thermal Engineering 67.1 (2014): 147-158".

This model enables to predict a future state of the Ecovat given the actual state and a control action, e.g. injection heat in a specific layer. An Ecovat loses thermal energy over time, to its environment and also to adjacent layers. This model is able to cope with these characteristics.

##### 2.1.1.1 Charging cycle

The parameters of the model were first estimated by a Newton-Gauss algorithm, and later by a Levenberg-Marquardt algorithm. This first did not always converge. During the first test the Ecovat was charged only.

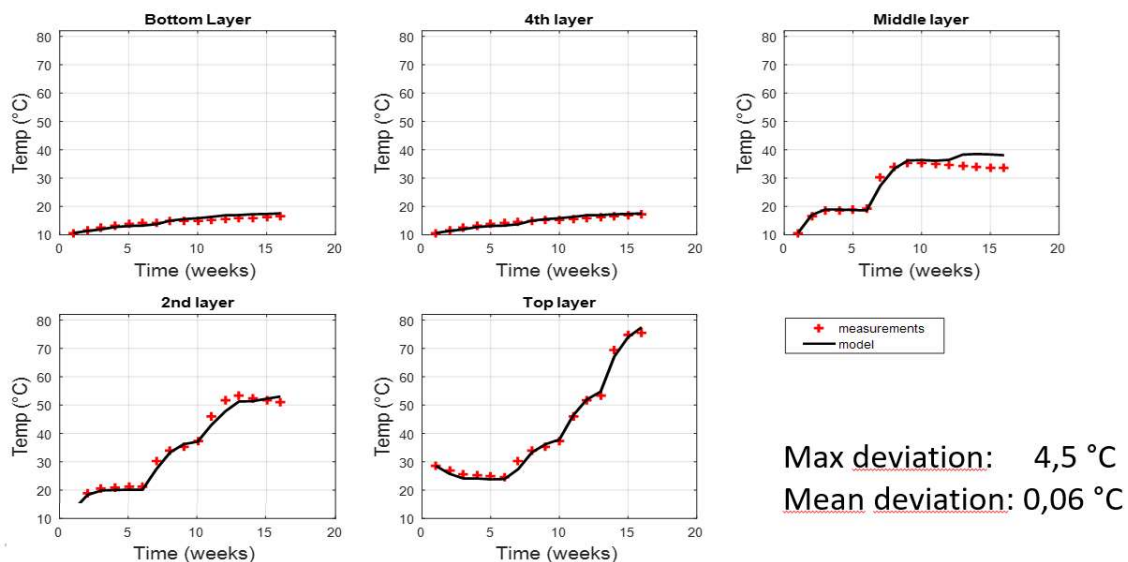


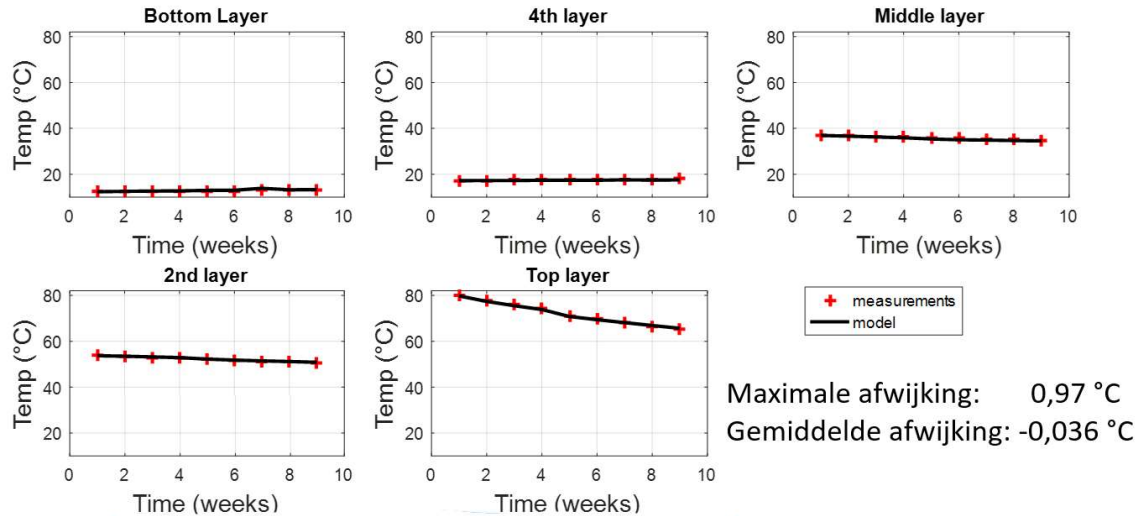
Figure 1: Charge test: measured vs. modeled temperatures

Figure 1 shows the results of the charge test. It was observed that:

- at the end of the test the measured values are slightly higher
- the fourth layers receives a little more heat than in reality
- the third layers cools down a little more than in reality

### 2.1.1.2 Discharging cycle

During the second test the Ecovat was discharged only.



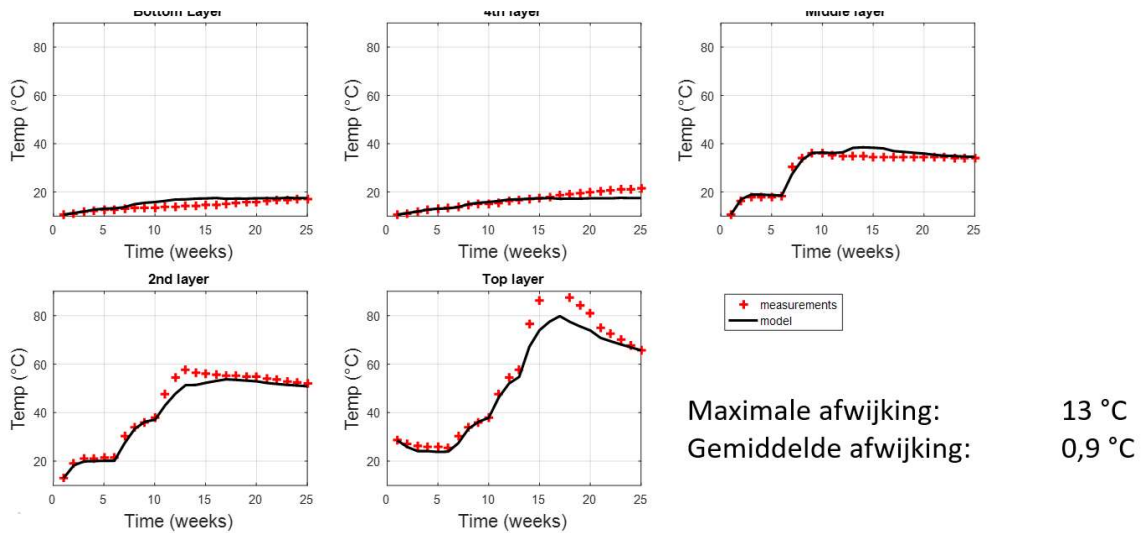
**Figure 2: Discharge test: measured vs. modeled temperatures**

Figure 2 shows the results of the discharge test. It was observed that:

- the model is very capable of describing the temperature evolution in the layers when no energy is added

### 2.1.1.3 Combined cycle

During the third test charging and discharging was combined.



**Figure 3: Combined test: measured vs. modeled temperatures**

Figure 3 shows the results of the combined test. It was observed that:

- The largest deviation was observed in the top layer. This is most probably caused by the heat added to the second layer moving to the top layer caused by convection.

#### 2.1.1.4 Recommendations from charging and discharging tests

From the observations and conclusions the following recommendations are derived:

- In contrast to earlier expectations, heat added to a particular layer will transfer to the top adjacent layer. This has to be taken into account when designing future control algorithms. Future algorithms will charge higher layers to a higher SOC than before, before charging the layers below.
- As expected, heat losses were higher than 10% over 6 months. This result will be taken into account in future vessels. These measurements will be used to calculate the optimal amount of insulation. The optimal amount of insulation will depend on i.a. the energy price, the duration of a single charge/discharge-cycle and the price of insulation.

#### 2.1.1.5 Failing Heat Exchanger

During the test period one of the heat exchangers in the Ecovatt vessel failed. This was detected by pressure test and by Fudura measurements. The P2H generators (heat pumps and resistors) were not able to work at their maximum power capacity, because the heat exchanger were not able to transfer all the generated heat to the vessel. This triggered the creation of an updated model and optimal control policy in order to cope with these problems.

### 2.1.2 The Heat pump signature model for indirect control

As we are using a standard off-the-shelf heatpump, the heat pump control to achieve (more or less) deterministic responses for profile following capabilities had to be done in an indirect manner by means of a temperature sensor override. Therefore, a HP signature model must be constructed (learned) that determines the optimal control (temperature sensor override value) profile for a given requested electricity consumption profile.

The HP signature model does this by learning the relationship between the power consumption and supply temperature, and combining this with the (learned) heating curve that gives the relationship between the supply temperature and the outdoor temperature sensor value (that is used as the heatpump indirect control signal).

#### 2.1.2.1 Training Data generation

We created 3 sets of training data to work with: a ramping up test, a ramping down test and a test with both ramping up and ramping down. Figure 4, Figure 6, and Figure 8 show the response of the electric power consumption and supply temperature to changes in the outdoor temperature sensor override in each of these tests. Figure 5, Figure 7, Figure 9 show the scatter plots of supply temperature vs outdoor temperature with a dark grey line superimposed to reflect the input heating curve that was set. Following observations can be made:

- The scatter plots of the outdoor temperature and the supply temperature agree with the set heating curve. The vertical spread is owing to the latencies involved in reacting to a change.
- When the outdoor temperature sensor value changes, the power consumption and supply temperature react to this change. In the ramping up test, in most cases, after an initial transient behaviour, steady state is reached.
- Ramping down is much less stable compared to ramping up.
- It can be noted from the 3 data sets that the transient behaviour to signals is not very uniform. Also, the time taken to reach steady state varies from case to case.
- The oscillatory and other transient behaviour are owing to the internal controller of the heat pump, which we do not have under control and of which we do not have knowledge (manufacturer private information).
- It can be seen from all the tests that there is a close dependency between the power consumption and the supply temperature. In most cases, there is no visible delay in the change in supply temperature w.r.t to changes in the power consumption.





**Figure 4: Ramping up test: the response of the electric power consumption and supply temperature to changes in the outdoor temperature override.**

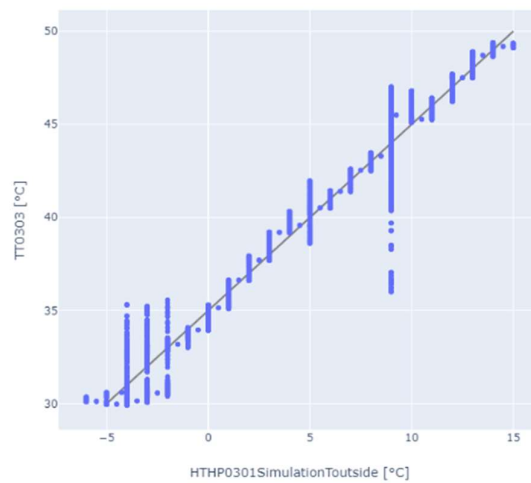


**Figure 5: Ramping up test: scatter plot of supply temperature vs outdoor temperature (the dark grey line superimposed to reflect the input heat curve).**



**Figure 6: Ramping down test: the response of the electric power consumption and supply temperature to changes in the outdoor temperature override.**

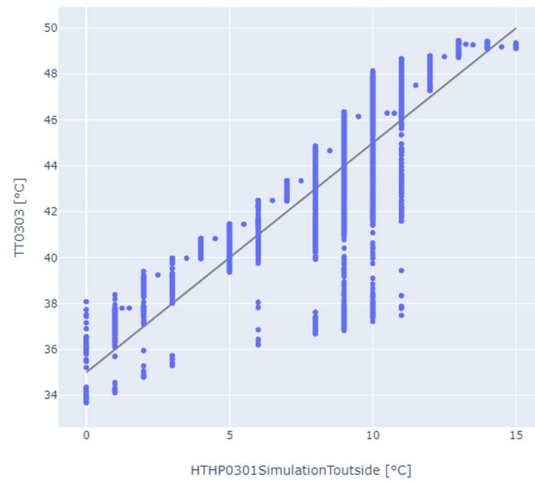


**Figure 7: Ramping down test: scatter plot of supply temperature vs outdoor temperature (the dark grey line superimposed to reflect the input heat curve).**

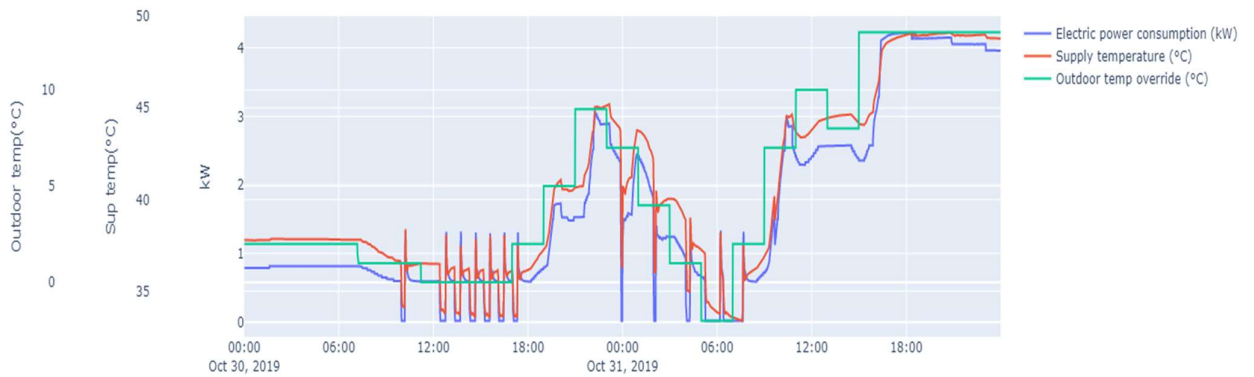


**Figure 8: Mixed test: the response of the electric power consumption and supply temperature to changes in the outdoor temperature override.**

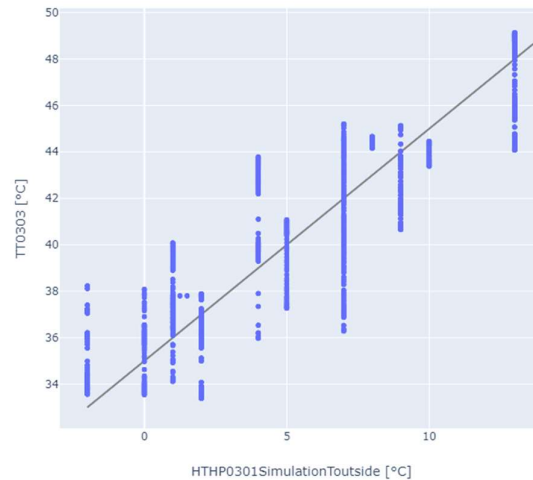


**Figure 9: Mixed test: scatter plot of supply temperature Vs outdoor temperature (the dark grey line superimposed to reflect the input heat curve).**

### 2.1.2.2 The HP signature model creation

The goal of the HP signature model, as stated above, is to give a HP control signal profile – i.e. as an outdoor temperature profile - for a requested power consumption profile that should be followed. To achieve this, we split the HP signature model into 3 components:

- Relation between power consumption and supply temperature
- Relation between supply temperature and outdoor temperature
- Time delay in the response of the supply temperature to the change in outdoor temperature.

The above split is motivated by the observations made before: the changes in supply temperature closely follows the changes in power consumption, the scatter plots reveal that the relation between the outdoor temperature and the supply temperature quite closely follows the input heat curve. The time delay is the most uncertain component above, and due of the lack of extensive data, we estimate a fixed value to use.

For the first component, we created a model of the relation between power and the supply temperature. We use a polynomial regression model for this, with the following features: the current power consumption, the power consumption from the previous time step and its squared, and the supply temperature (on the primary/evaporator side of the heat pump. For training this model, we used part of the data from the ramping up test (i.e. until the 18<sup>th</sup> of October). We validated the model using three data sets: the rest of the data from the ramping up test, the ramping down test and the mixed test. The accuracies in terms of the root mean

square error (RMSE) and the symmetric mean absolute percentage error (sMAPE) of each of the cases are presented in the table below.

Case/indicator	RMSE	sMAPE
<b>Training</b>	0.05 °C	0.01 %
<b>Validation, ramp up</b>	0.79 °C	1.04 %
<b>Validation, ramp down</b>	0.62 °C	1.0 %
<b>Validation, mixed</b>	0.62 °C	1.2 %

**Table 1: The training and validation errors for the model that learns the relation between the power consumption and supply temperature**

From Table 1, Figure 10, Figure 11, Figure 12 and Figure 13 we see that this model is of acceptable accuracy. Thus, for a given target power consumption, we know the target supply temperature should be requested.

For the second component, the heating curve (either modelled from measurements as in Figures 2, 4, 6, or from the known HP setting), we know for a requested target supply temperature, what the outdoor temperature setting should be (which override value will be the HP indirect control signal).

For the third component however, as stated earlier, the time delays and transient behaviours are the most difficult to capture:

- The delay in reaction to a control signal is unpredictable
- The ramp up/down rates are very slow
- There are many unexplained transient reactions to the control signal, which leads to non-deterministic behaviour that makes the offering of fine-granular profile following services very difficult.

As seen in Figure 14, the power consumption in some cases takes 2–3 hours to reach steady state. In other figures we can see that the power consumption in some cases starts to change immediately after a control signal, or sometime takes close to 1 hour to start changing (transient and ramping up apart). Hence, we decided on a test case where the calculated outdoor temperature is given 1 hour in advance as and where the requested power consumption profile (that embeds a flex offering) does not change very rapidly. This takes into account the HP intrinsic limitations, which in this case limits flex service offerings to coarse grain profiles.

It is clear that this indirect control paradigm is hampered by the HP internal controller decisions that impacts (i.e. worsens) the deterministic behaviour (i.e. power consumption) of the heatpump in response to an indirect control signal. Current results indicate that through more sophisticated modelling, the level of determinism could be further improved though. Especially if done in concertation with improvements of the internal controllers to make them better fit for offering flexibility. The Grid Flex Heatpump experiments conducted in T2.4 have shown that the 'flex' characteristics of heat pumps differ vastly between different brands and models, and that some models are better fit for (indirect) flex control than others.





**Figure 10: The data used to train the heat pump model, and the resulting fitted values.**

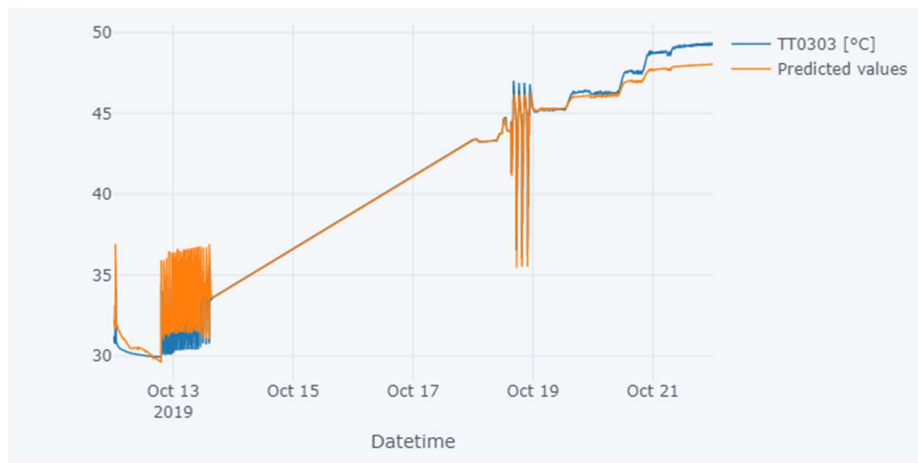


**Figure 11: Validation of the model for a part of data in the ramping up test.**



**Figure 12: Validation of the model in ramping down test.**

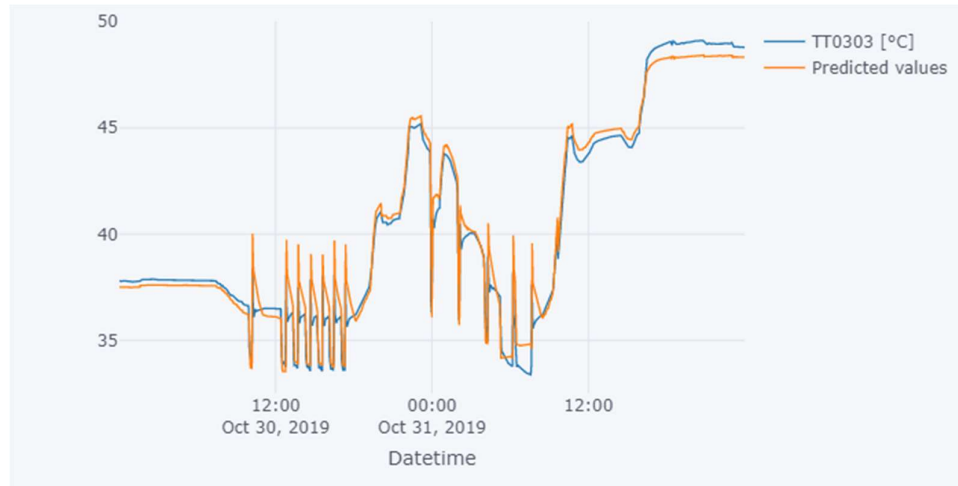


**Figure 13: Validation on the data from the mixed test.**



**Figure 14: A zoomed in version of the ramp up test, to focus on the delays in response of the supply temperature to change in outdoor temperature.**

## 2.2 Demand profile following capabilities

### 2.2.1 Test profile

In Figure 15, we show one of the test profiles for the Ecovat heatpump. It shows the heat pump's requested power consumption profile (blue curve) which could relate to a (block-wave) service offering profile. As learned from T2.4, the flex capabilities from heat pumps – determined by their internal controller – differ vastly between different brands and models. To take into account the specific capabilities of the Heatpump that was installed in the Ecovat, we have restricted the test power consumption profile to not vary too rapidly (i.e. the block time step granularity in this case is 4 hours; but as can be seen from the experiments from T2.4, this can be much smaller if a better suited heatpump is available).

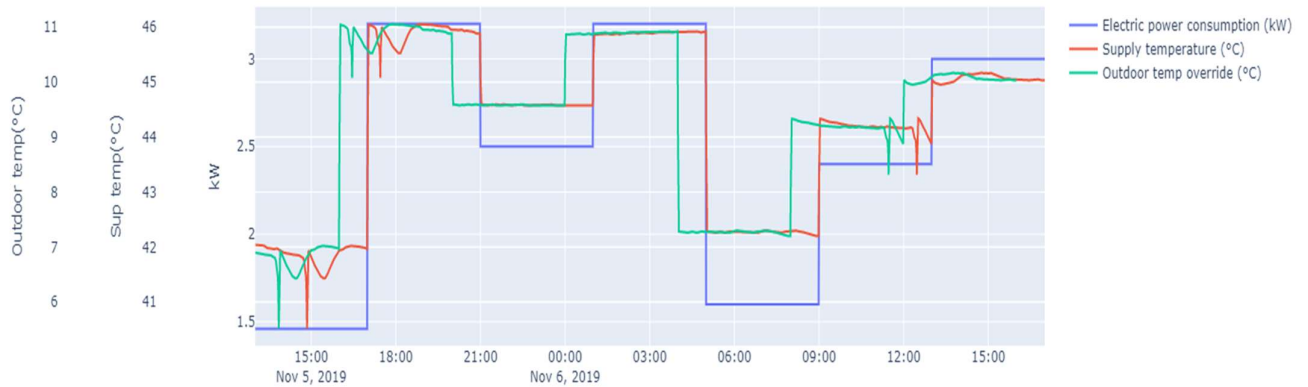


**Figure 15: Test profile for the heat pump.**

As described in section 2.1.2.2, for a given target power consumption profile (blue curve), a corresponding supply temperature profile is derived using component 1 of the HP signature model (red curve). Next, this supply temperature profile is converted into the HP control signal profile (i.e. outdoor temperature override profile: the green curve) using the heating curve (model). To take into account the latency between the HP control signal and the heatpump response, the HP control signal is given with some lead-time: in this experiment, an average lead-time of one hour has been used.

### 2.2.2 Analysis

In Figure 16, we show the measured values of the supply temperature and power consumption in response to the HP control signal (outdoor temperature override). In Figure 17 and Figure 18, we show the target power consumption profile and derived target supply temperature profile against the actuals respectively. The following observations are made.

- The response to the HP control signal is as expected in many of the cases – both in power consumption and supply temperature.
- The target power levels are mostly in agreement in the steps that need a ramping up.
- The steps that need a ramping down are less predictable.
- The delay in the response to the control signal is unpredictable. While in some cases the heatpump starts ramping up/down immediately, there are other cases where it could take up to an hour to start reacting. Multiple factors contribute to this delay: e.g. the delta between the current supply temperature and the target one, the amount of heat that can be delivered (i.e. thermostats that may block heat delivery), and the internal heatpump controller logic. It is anticipated that by added more sophistication to the HP signature model, also these delays can be modelled with more accuracy to improve the overall accuracy of the indirect control approach. This will be further explored in future research projects.

- The (mostly small) difference in the achieved stable levels could be owing to the HP signature model inaccuracies, as well as to the deviation in the forecast of the input temperature to the primary side of the heat pump (T202).



**Figure 16: The response of the electric power consumption and supply temperature to the control signal.**



**Figure 17: Planned consumption (blue) vs actual consumption(orange).**

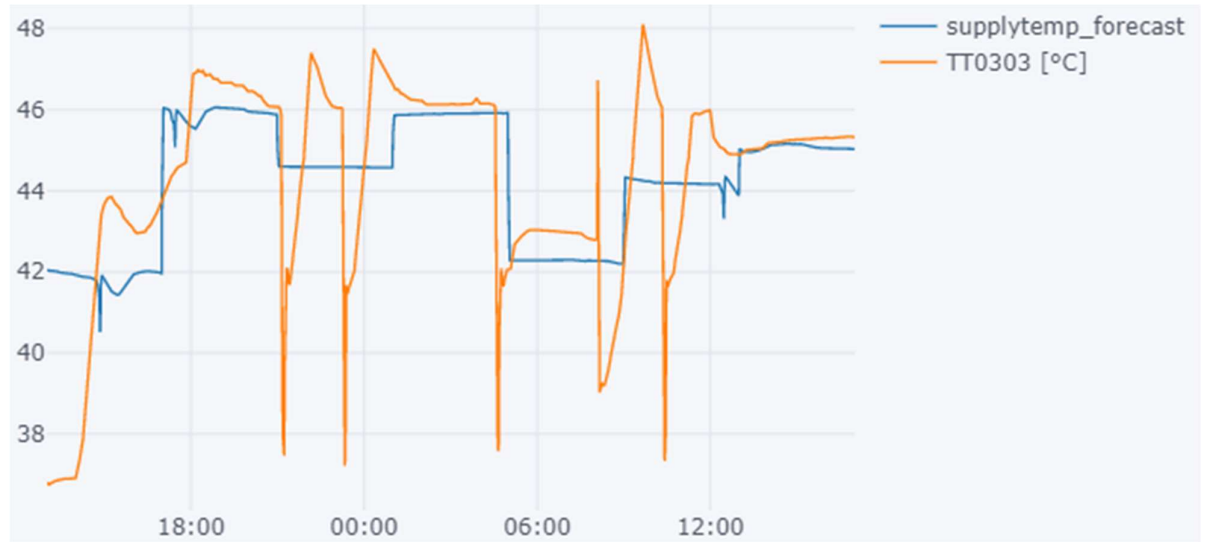


**Figure 18: Planned supply temperature(blue) vs actual supply temperature(orange).**

Table 1 below summarizes the deviation between the planned and actually consumed energy for a 4hr service time block (e.g. for a RES curtailment mitigation service).

Service time block (4hr resolution)	Energy planned (kWh)	Energy consumed (kWh)	Deviation (%)
13:00:00 — 17:00:00	5,87	6,62	12,78%
17:00:00 — 21:00:00	12,84	12,25	4,60%
21:00:00 — 01:00:00	10,05	10,59	5,37%
01:00:00 — 05:00:00	12,83	11,16	13,02%
05:00:00 — 09:00:00	6,44	6,89	6,99%
09:00:00 — 13:00:00	9,65	10,55	9,33%
13:00:00 — 17:00:00	12,05	10,27	14,77%
		<b>Average Deviation</b>	<b>9,55%</b>

**Table 2: Error quantification for a 4hr timestep curtailment mitigation service.**

### 3 Swedish Pilot, VITO building agent services

#### 3.1 Model Accuracy

##### 3.1.1 The heatpump signature model for indirect control

In the Swedish pilot, the desired HP power consumption values were set through the NODA API, which translated them to outdoor temperature override values for the indirect HP control. For this translation, the NODA platform has created a heatpump signature model that models the relationship between the heatpump power consumption (as a result) and the outdoor temperature sensor value (the control input). This heatpump signature model was created by NODA based on regular measurements that are available from the buildings using the standard (thermostatic) controller. I.e. no specific perturbations to collect a richer data set were done in order to not expose the tenants to possible discomfort conditions, and to mimic a deployment scenario where the signature model creation would be done based on regular historical data.

Figure 19 illustrates the heatpump signature model for one of the pilot buildings. The heatpump signature, i.e., the regression line, was computed by the method of ordinary least squares from the (historical) measurement data.

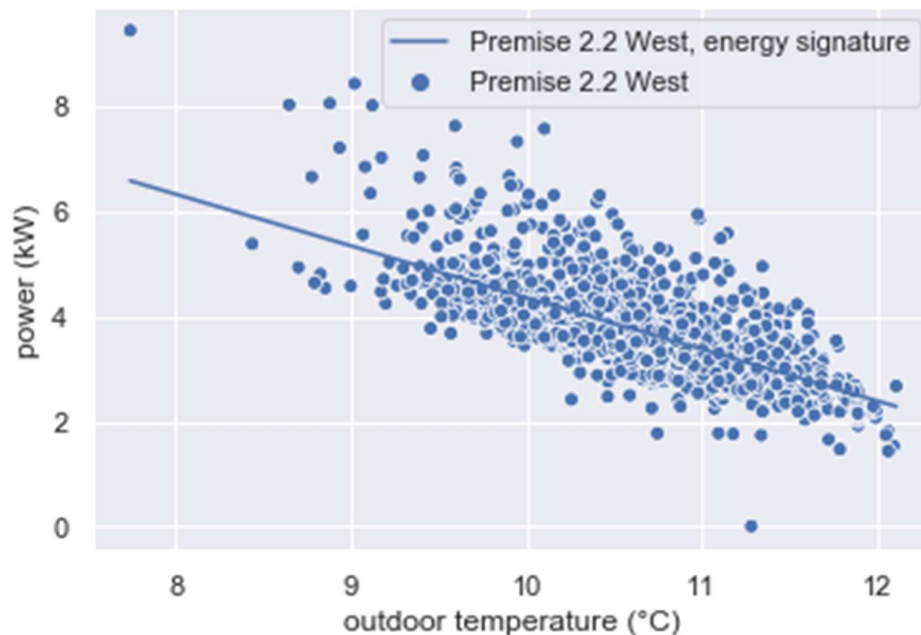


**Figure 19: Heatpump signature for P1.2 (West), computed over three months of hourly data.**

This specific building, Premise 1.2, is a hangar operated by a logistics company. One of the important contributing reasons for the data points spread around the

regression line, is due to the specific operation of the hangar, with frequent and irregular opening and closing of the loading bay gates.

Similar spreads can be seen for the residential buildings. There, one of the important contributing reasons for the data points spread around the regression line, is the inability to distinguish between the heatpump running for space heating versus running for DHW generation (next to user behaviour impact like opening/closing doors or windows, or changing thermostat setpoints). As a rule of thumb, the use of DHW is responsible for 20-30 % of the heat demand for residential buildings, with larger numbers for better insulated buildings, and constitute a more or less irreducible source of uncertainty when attempting to predict the energy consumption. The situation is complicated by the fact that they have their own control system subject to the (local) legal framework for Legionella. From this, it is clear that explicit and separate control – and data – of space heating cycles versus DHW heating cycles has the potential to eliminate at least part of the uncertainties. To enable this, a data analytics approach has been developed that uses temperature measurements of piping to distinguish between HP running for DHW versus HP running for space heating.

### 3.1.2 The building dynamic thermal model

In this section, some results of pilot building thermal model training are presented. For more information about the building thermal models used, and the process of data collection for model training, please refer to deliverables from work T2.2 and T4.4 respectively.

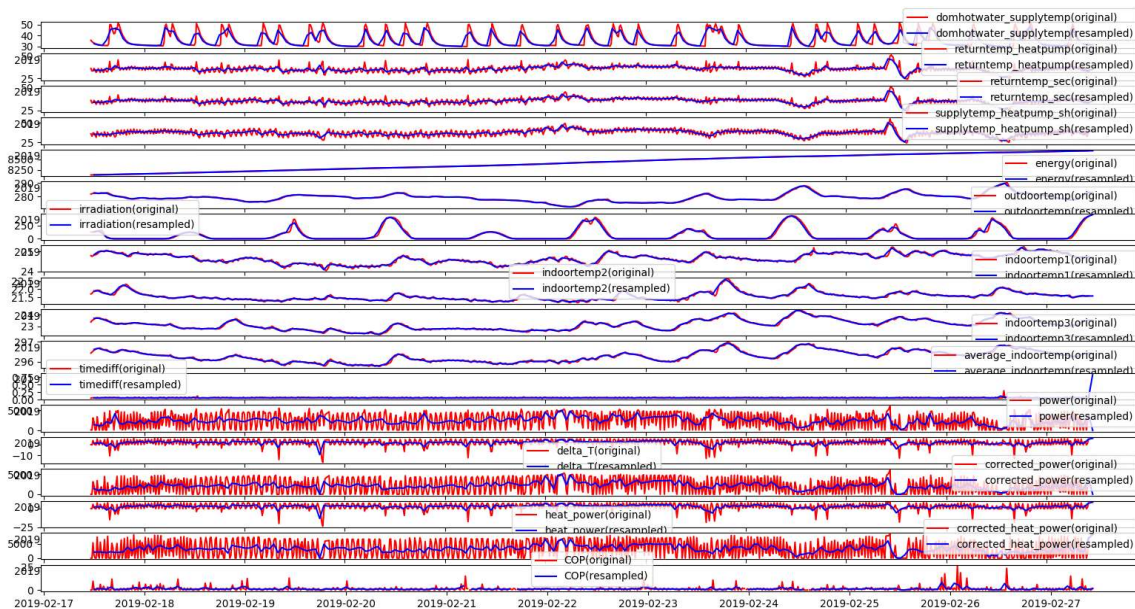
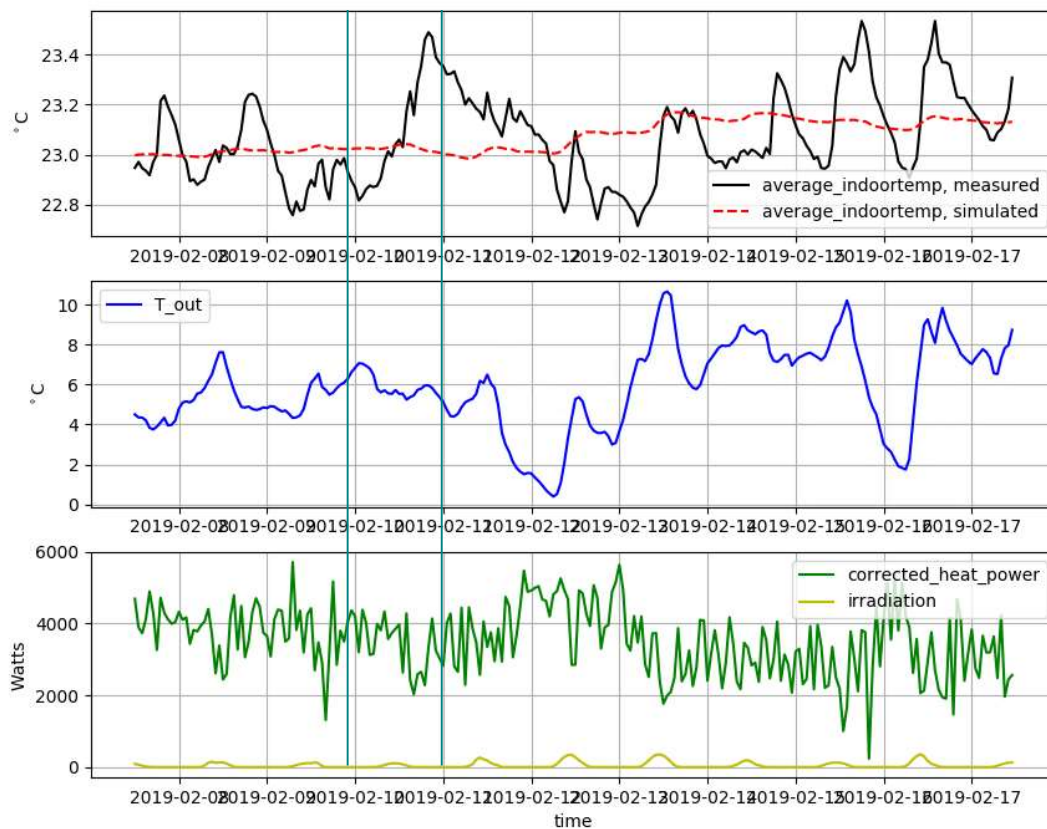


Figure 20: Input data for P2.1 (residential building).



The data in Figure 20 shows a 10-day period for Premise 2.1 that was used for fitting the building grey-box model RC parameters. The data was split in two parts of 5 days for auto-validation and 5 days for cross-validation. The corrected\_power and corrected\_heat\_power values are values that represent space heating cycles only i.e. filtering out DHW generation cycles, using a methodology that was created to distinguish between the two cycles based on data coming from piping temperature sensors. The resampling values are values resulting from a data cleaning process that corrects for missing or irregularly spaced data samples and for timestamp mismatches between data coming from different sensors or meters. This is needed in order to correctly correlate the data coming from different data sources. Specifically for the power values, it as well ensures that the time integration of the resulting power value samples matches the corresponding energy measurements over the corresponding time intervals.



**Figure 21: Results of auto-validation fitting for P2.1 (residential building).**

The fitting process does not result in a model that is able to predict the short-term dynamic behavior of the building: the simulated (forecasted) temperature profile does not correlate well with the measured temperature profile (top pane, Figure 21). Although the absolute error is rather small, the short term dynamics are lacking. This is due to the fact that for the data collection to fit the RC parameters,

no perturbations – to collect more rich training data – could be done. Actually, when there as well is thermostat control (as was the case in our pilot buildings) even if perturbations would have been done at the heatpump level, this may not have led to more variations of the indoor temperature in the training data, as this would have been prevented by the thermostat control in the apartments that aims at keeping a (more or less) constant temperature, and would prevent specifically temperature increases even if the HP is perturbed with the intention to increase the indoor temperature. On the other hand, higher indoor temperatures might be observed due to internal gains or irradiation that cannot be blocked by the thermostat, yet not correlated with the HP behavior.

During this 10-day period the indoor temperature ranges between 22.8 °C and 23.4 °C. Additionally, the provided heat\_power shows rapid oscillations, but considering the thermal inertia of buildings, the impact of these rapid heat\_power oscillations are in general averaged out and rarely visible. The result of the fitting procedure is therefore a model that reproduces the general trends of the indoor temperature in correlation with the average heat-power that is supplied: it provides an R value that represents the thermal losses to the ambient which are compensated by the heat delivered by the heat pump. Deviations from this can be observed, that are related to unknown factors like for instance internal gains. This is for instance particularly evident in the indicated zone where a rapid increase of the indoor temperature can be observed, without any changes in the ambient temperature, heat\_power or solar irradiation. Because of these reasons, sensitivity to the value of C, the thermal mass of the zone, is therefore limited in this case.

Fitting building model parameters using this kind of in-use data – where no perturbations can be done – should therefore be done with care. It is recommended to try to gather training data which includes sufficient data on the thermal dynamics of the building. This can be achieved by using a pseudo-random binary control signal for the heat pump. This control sequence is apparently random despite the fact that it is fact deterministic and includes a wide range of frequencies. This however would only be possible to the extent that a controller at the heat delivery side – e.g. a thermostat – would not be limiting the temperature deviations.

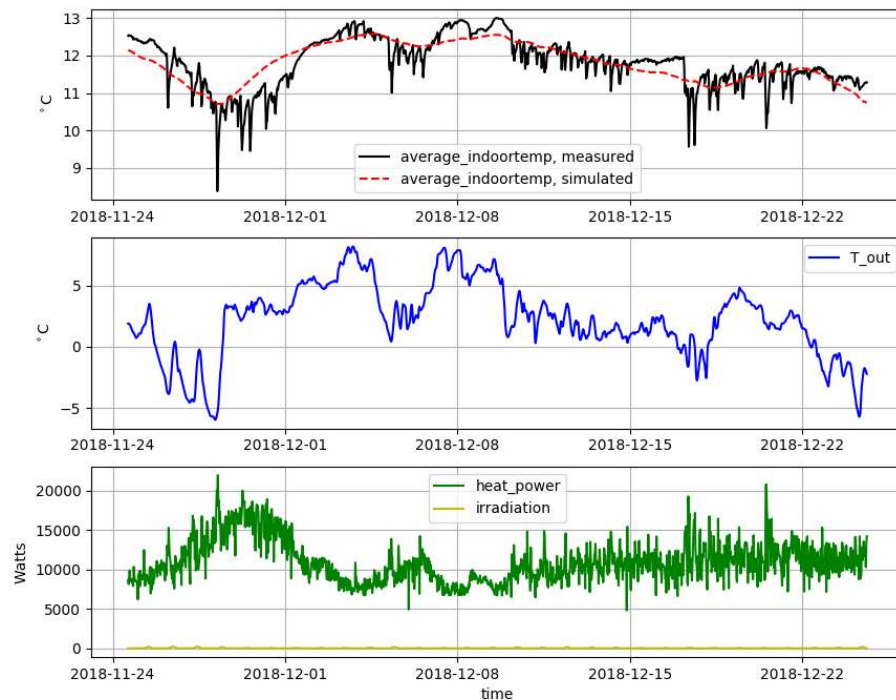


**Figure 22: Fitted results from P1.2 (East) (industrial building).**

Premise 1.2 (East) is a part of a hangar which exhibits a very distinct temperature profile. In contrast with the example of Premise 2.1, the indoor temperature shows more variations, namely between 8.5 °C and 13 °C. Striking are the rapid temperature swings that are observed. These are most probably caused by opening the doors or gates of the building since they occur in a distinct pattern following weekdays. Week-ends show a flatter behavior. Also here, the model shows a good overall reproduction of the indoor temperature apart from the rapid swings that are probably due to the gate openings. Though the fitted values for R and C include these effects in an average way. One should also consider the influence of temperature sensor position. When the indoor temperature sensor is located near a gate or door which is opened at regular times, the recorded temperatures are not representative for the whole thermal zone.

The cross validation shown in Figure 23, especially the first days, does not seem very accurate. This is explained by the fact that the cross-validation period starts around Christmas time - i.e. holiday season without frequent opening of the gates. Therefore it does not show the rapid oscillations of the indoor temperature, and the average indoor temperature is significantly higher than the simulated one, due to the fact that there are less heat losses because of this as well. When the work got resumed after the holiday season, it can be seen that the error becomes smaller again, and the indoor temperature oscillations resulting from the gate openings become visible again.

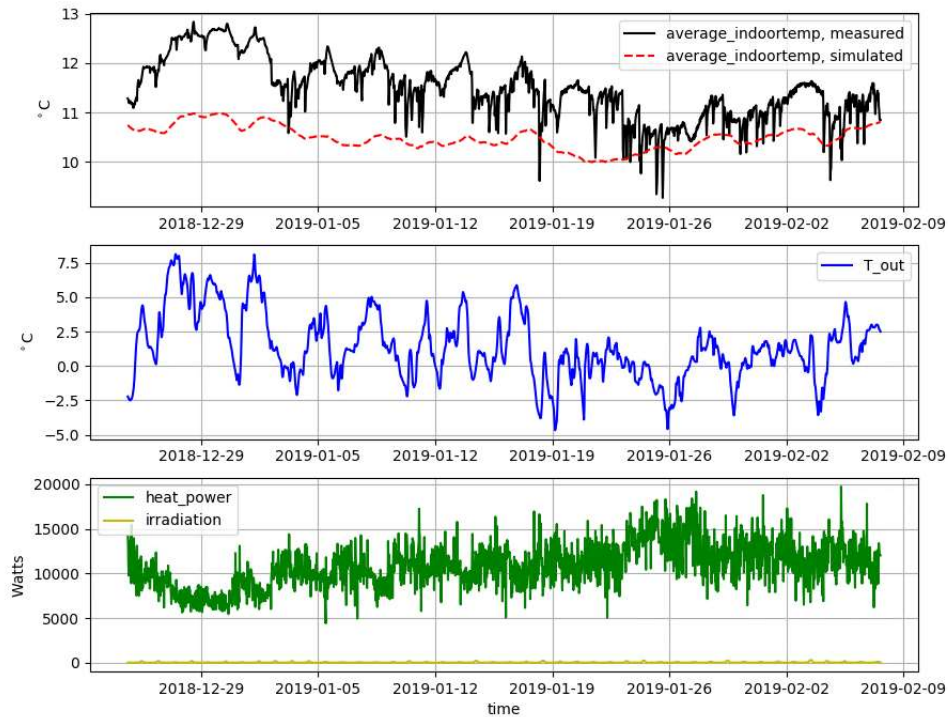


**Figure 23: P1.2 (East) cross validation results (industrial building).**

The results for the third premise, Premise 2.3, are shown in Figure 24. The indoor temperature is also confined to a narrow range (by the thermostat), similar to the situation in Premise 2.1 (Figure 21). The simulated indoor temperature reproduces the measured data in a very good manner.

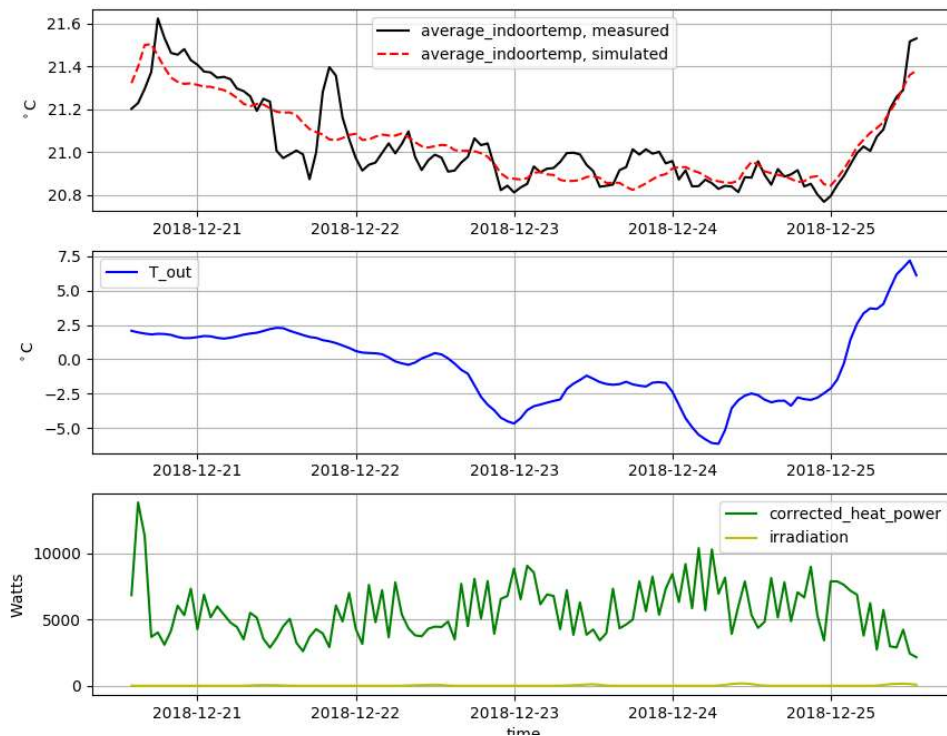


Figure 24: Fitted P2.3 results

### 3.1.2.1.1 Model training error metrics

To summarize, Table 3 gives an overview of the different RMSE that were observed when comparing the measured average<sup>3</sup> indoor temperature of the buildings with the simulated average indoor temperature (both for auto-validation and cross-validation).

Premise	RMSE, auto	RMSE, cross
P2.1	0.294	0.770
P1.2 (East)	1.869	1.349
P2.3	0.346	-

Table 3: RMSE of building model training

### 3.1.3 Quality of exogenous parameters

The ability of the FHP solution to perform demand profile following depends on its ability to predict electricity demand, which in turns depend on future weather conditions, for example the building-specific outdoor temperature and the building-

<sup>3</sup> As there was no monitoring or control of the individual apartment thermostats nor heat delivery, a single zone modelling was done using an indoor temperature which is the average of the indoor temperatures of the three apartments. This proved to be work reasonably well, taking into account the many other uncertainties in the retrofit expert-free approach that we applied.

specific cloud coverage. To this end, the FHP pilot validation relied on data from Yr<sup>4</sup>, the joint online weather service from the Norwegian Meteorological Institute<sup>5</sup> and the Norwegian Broadcasting Corporation (NRK). Yr is unique in Europe because of its highly detailed weather forecasts and its free data policy.

While is impossible for anything but another meteorological institute to improve on the weather forecasts from Yr, it is nevertheless possible to improve on the forecasts of the building-specific outdoor temperature by means of machine learning. Analysis of the local outdoor temperatures from buildings in Karlshamn, Sweden, suggests the possibility to improve on the accuracy and the precision of the forecasts to some degree, see Figure 25. However, the lack of building-specific daylight sensors makes it difficult to improve on the forecasts of cloud coverage, although the growth of photovoltaics can provide a solution.

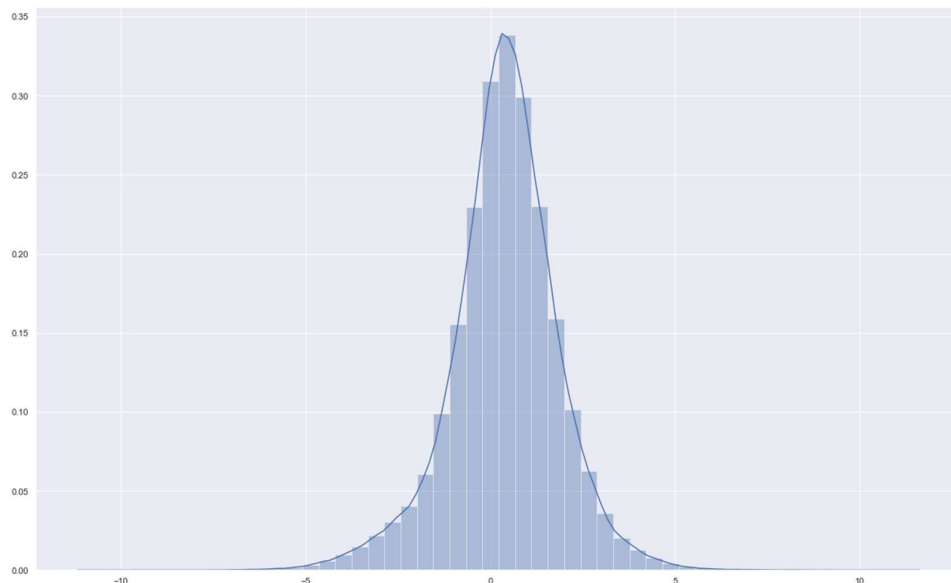


**Figure 25: Distribution of the accuracy of the forecasted outdoor temperatures in Karlshamn, Sweden, with mean 0.4 °C and standard deviation 1.5 °C**

### 3.1.4 Quality of sensor data

The indoor temperature sensors (CMA12w, Elvaco) use the wireless M-bus protocol to communicate with a master unit, which in turn uses GPRS to communicate with the NODA cloud. The sensors have a measurement range from -20 to 55 °C, and high accuracy with a margin of error of  $\pm 0.2$  °C for the range from -20 to 5 °C and a margin of error of  $\pm 0.4$  °C for the range from 5 to 55 °C. The inappropriate placement of the sensors can result in biased measurements. Consequently, they should not be installed in locations that are often exposed to direct sunlight, nor close to sources of heat and cold.

<sup>4</sup> <https://www.yr.no>

<sup>5</sup> <https://www.met.no>

The pipe temperature sensors (VFG54 LON, Thermokon-Danelko) that measure supply and return temperatures are [clamp-on] contact temperature sensors. This means that they measure the temperature on the outside of the pipe, and not the temperature of the media inside the pipe. Consequently, the accuracy is lower than for a comparable sensor located inside the pipe. However, [clamp-on] contact sensors pose a cost-effective solution comparable to invasive sensors. And although the accuracy is less, the precision is still high enough to capture the dynamics of the temperature of the media inside the pipe.

### 3.2 Demand profile following capabilities

#### 3.2.1 Background

The building dynamic thermal models that were discussed in the previous section are used to determine optimal power consumption profiles. To relate thermal power to electrical power, RISE has supplied affine models of COP and VITO has integrated these models of the COP with their thermal models to the end of computing a power profile describing the desired power consumption a heat pump. It would be more accurate to model COP by a nonlinear function of the historical heat demand. However, the resulting nonlinear model of power consumption would preclude the FHP ADMM optimisation algorithm for mathematical reasons. And with the objective of keeping the involved computations energy efficient, as not to counteract the purpose of the FHP project, it is difficult to improve on the model.

Table 4 provides an overview of the four tests that were conducted with the buildings of the Swedish pilot. For each of these tests, the full end-to-end chain was tested based on the local Renewable Energy Source (RES) curtailment use cases as defined in D1.1 (Dominguez, Rivero, Caerts, & Brage, 2017).

ID	Premises	Description
<b>No_Flex</b>	P2.1, P2.3, P1.2 (E, W)	No Flex Request from DSO: building flex is used for determining own optimal consumption plan.
<b>Flex_1</b>	P2.1, P2.3, P1.2 (E)	Flex Request from DSO
<b>Flex_2</b>	P2.1, P2.3, P1.2 (E)	Same as Flex_1, but with improved comfort boundary modelling.
<b>Flex_3</b>	P2.1, P2.3, P1.2 (E)	Same as Flex_2, but with improved building models and applying a shorter rolling horizon approach.

**Table 4: Overview of selected tests in Swedish pilot**

Before conducting these cluster tests, the premises were individually tested to ensure a fully operational end-to-end chain. Further information about the premises subject to these tests can be found in (Brage, et al., 2018).

In the first test that was conducted – No\_Flex –, no local RES curtailment was forecasted by the DSO. Therefore, the DSO accepted the baseline consumption profile of the cluster, and no flexibility requests were made by the DSO to the DCM (and by the DCM to the buildings). This means that the buildings requested power profile (i.e. building control signal) is identical to the optimal baseline consumption plan they constructed for themselves.

During the following three tests – Flex\_1 to Flex\_3 –, local RES curtailment was forecasted by the DSO and a corresponding flexibility request was sent to the buildings. Subsequent learnings and improvements were gradually introduced between in each of these tests.

### 3.2.2 Analysis

#### 3.2.2.1 No\_Flex

In this test no local RES curtailment was forecasted, and the DSO accepted the cluster's aggregated baseline consumption profile as is. This test was used to analyse the individual behaviour of the buildings based on the control signals their heat pumps receive from our control algorithm, e.g. how well are we able to follow an optimal profile that the building determined for itself.

In order to analyse the results of this test the following quantities were compared:

- For each building: building control signal<sup>6</sup> (= planned power consumption profile) and actual power consumption profile.
- For the cluster: The aggregated planned consumption profile and the aggregated actual power consumption profile.

Table 5 presents various performance indicators for the different pairs of quantities:

- The correlation coefficient (where 1 means perfect linear dependence, -1 is negative linear dependence, and 0 means no correlation).
- The p-value for a statistical test independence where the null hypothesis is that the quantities of interest are probabilistically independent of one another. With a low p-value ( $< 0.05$ ), the null hypothesis can be rejected (with 95% significance), and otherwise not.
- The sMAPE calculated as

---

<sup>6</sup> In the remainder of this document, we distinguish between the building control signal (NODA API terminology) and heatpump control signal. The building control signal is the power consumption profile we want the building (more specifically: the heatpump for space heating) to follow. The heatpump control signal is the indirect control signal (i.e. the outdoor temperature sensor override value) that is sent to the heatpump.

$$\frac{2(y - x)}{x + y}$$

Quantities	Correlation	p-value	sMAPE
<b>P1.2 (East)</b>	0.95	0.000	25.3 %
<b>P1.2 (West)</b>	0.84	0.170	48.0 %
<b>P2.1</b>	0.96	0.000	13.7 %
<b>P2.3</b>	0.95	0.005	17.7 %
<b>Aggregated</b>	0.95	0.035	27.8 %

**Table 5: Performance indicators of the individual buildings for the No\_Flex test.**

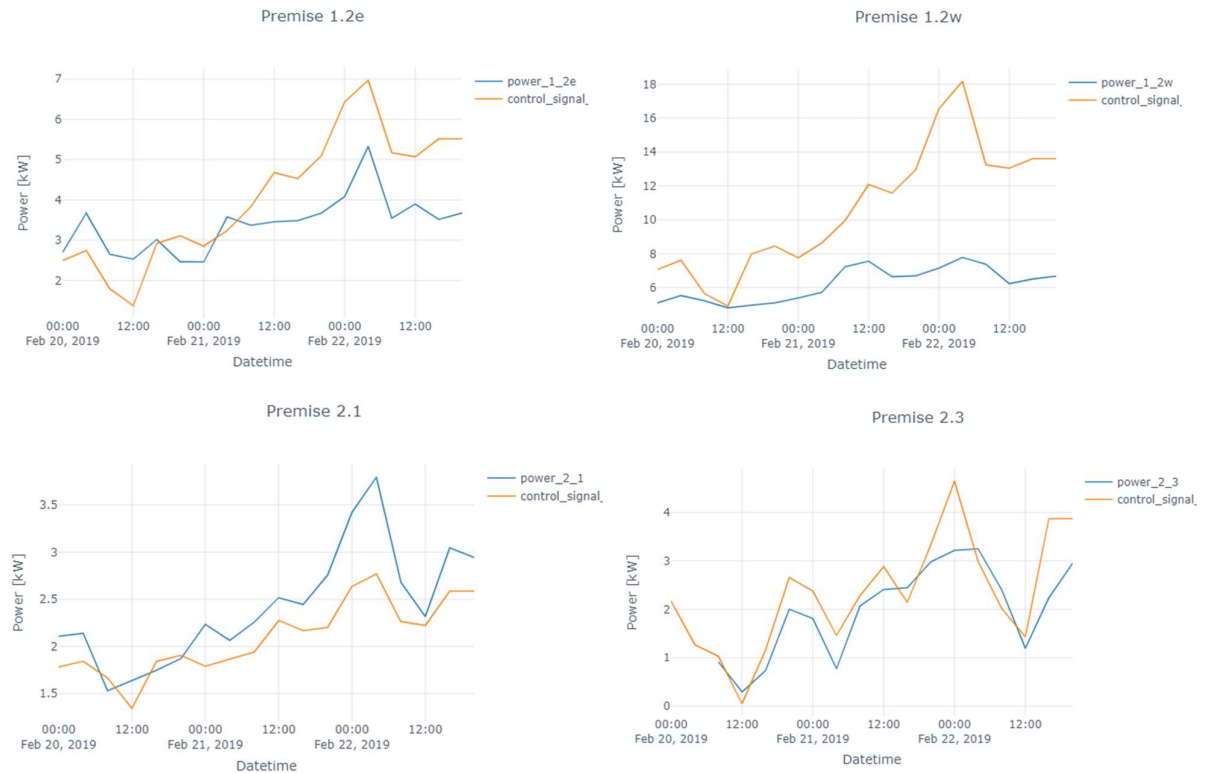
It can be observed that all the signal pairs have a good correlation coefficient. From the sMAPE, we can see that in particular the residential premises 2.1 and 2.3 show more potential for controllability as their sMAPE is significantly smaller than that of the other buildings. However, from both Table 5 and Figure 26 it is evident that the control of specifically the west wing of premise 1.2 is not as expected. This is partially due to the unpredictable gate openings and closing and the impact thereof on the indoor temperature. Furthermore, the corresponding heatpump could only be controlled by overriding the indoor sensor, rather than the outdoor sensor which was the control strategy that was selected in WP2. Therefore this premise P1.2 (West) was left out for the Flex\_1 – Flex\_3 tests.

Figure 26 shows the building control signal (i.e. requested consumption profile) that was sent to the different buildings together with the actual power consumption of the buildings. The data in these graphs are rolling averages to visualize the trend of the power consumption of the building. As a reference Figure 27 shows the same comparison for premise 2.1 but using 5 minute sampled values. It can be seen that the particular heatpump at hand showed mainly on/off behaviour for which it is difficult to correlate this with a more smooth curtailment mitigating building control signal. For the specific heat pumps in this retrofit context, no fine-granular profile following behaviour could be achieved, which of course has an impact on the flexibility services that it can offer to the market. However as shown in D2.3 (Lindahl, et al., 2018) other brands and models of heat pumps are able to follow more dynamic requested power profiles without showing in a more accurate and deterministic manner. In line with the limitations of the heat pumps at hand, and the associated possible services, the remainder of this document will show the 4 hour averaged graphs in order to hide the cluttering of the on/off modulation of these heat pumps.

To determine the building’s safe control signal, the comfort boundaries must be known. In the retrofit context were we were operating, we must take into account that next to the heatpump control that we do (heat push control) there is a second unknown thermostat controller (heat pull control) that may block heat delivery in



case the heatpump would be delivering too much heat. Therefore, in line with our expert-free ambition, we try to model the thermostat characteristic based on measurements to derive based from this comfort boundaries (that would trigger thermostat interventions) that are subsequently taken into account when calculating the flex boundaries within which the optimal consumption plan is determined.



**Figure 26: Comparison building control signal<sup>7</sup> and actual power consumption of the buildings in test No\_Flex (4-hour average).**

<sup>7</sup> Building control signal is target HP power consumption profile (not to be confused with the HP control signal, which is an outdoor temperature override profile).

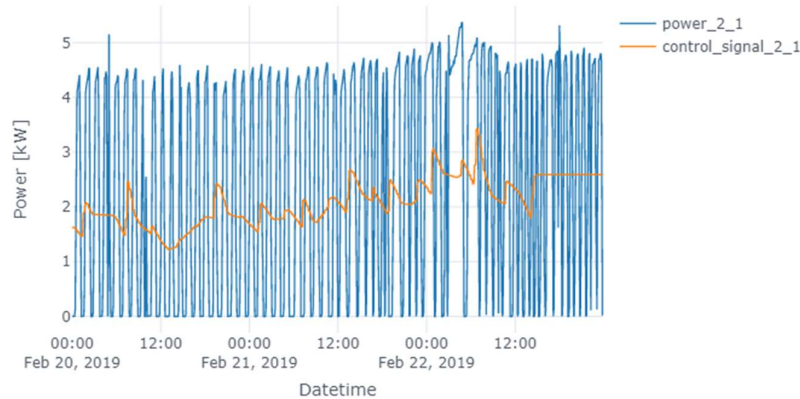


**Figure 27: Comparison building control signal and actual power consumption of P2.1 (5-min average)**

In Figure 28 it is shown that the building and heatpump control signals applied during this test kept the indoor temperature of the four buildings within, or close to, their respective comfort bounds. It can be seen though that for P2.1 the indoor temperature is mostly slightly below the lower comfort boundary.

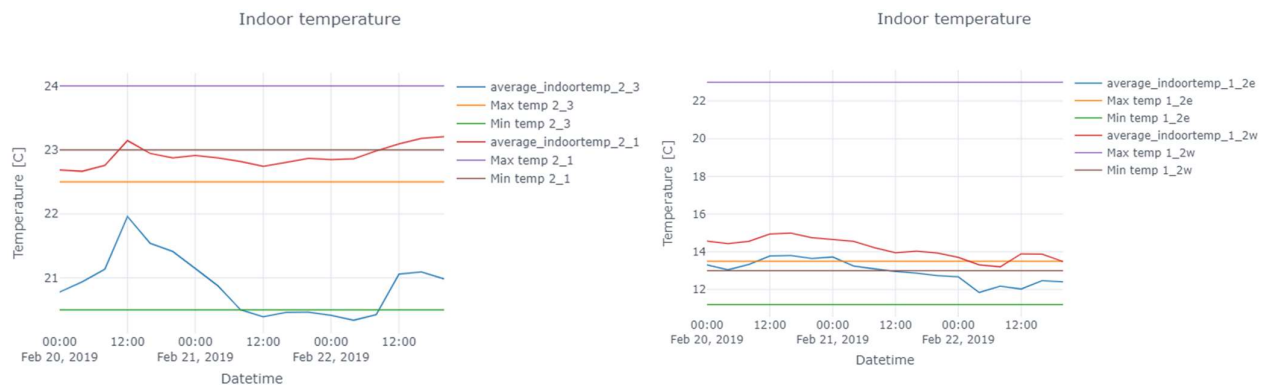


**Figure 28: Average indoor temperature and comfort boundaries.**

There are multiple sources for the error that is incurred:

- The internal controller of the heat pump
- The HP signature model (that translates the required power to a temperature offset for indirect control of heat pumps)
- The estimated/modelled comfort boundaries (relate to thermostat characteristics)
- The grey box models (this is an approximation and thus doesn't captures the building's behavior in all detail)
- The HP COP model

### 3.2.2.2 Flex\_1 and Flex\_2

The first full integration test with real flexibility requests coming in from the DSO was called Flex\_1. E.g. there is a flexibility request to the cluster of buildings to increase their combined consumption with 4 kW during 4 hours from 10:00 to 14:00. The analysis of the actual versus requested power consumption in Figure 29 showed that the actual power consumption profile of especially Premise 2.1 and Premise 1.2 (East) were not as expected. Analysis of the data showed that there was an error in the comfort boundaries setting of these buildings. After making corrections to the comfort boundary settings and rerunning tests (FLEX\_2), Figure 30 gives an overview of the building control signals and the corresponding power consumption of the three buildings. Premise 2.1 and Premise 2.3 are following the trend of the requested power quite well in contrast to Premise 1.2 (East). However, looking at the overall power consumption profile of the cluster shown in Figure 31, we see that it is following the trend of the planned cluster power profile.



**Figure 29: Comparison building control signal<sup>8</sup> and actual power consumption of the buildings in test Flex\_1 (4-hour average).**

<sup>8</sup> Building control signal is target HP power consumption profile (not to be confused with the HP control signal, which is an outdoor temperature override profile).

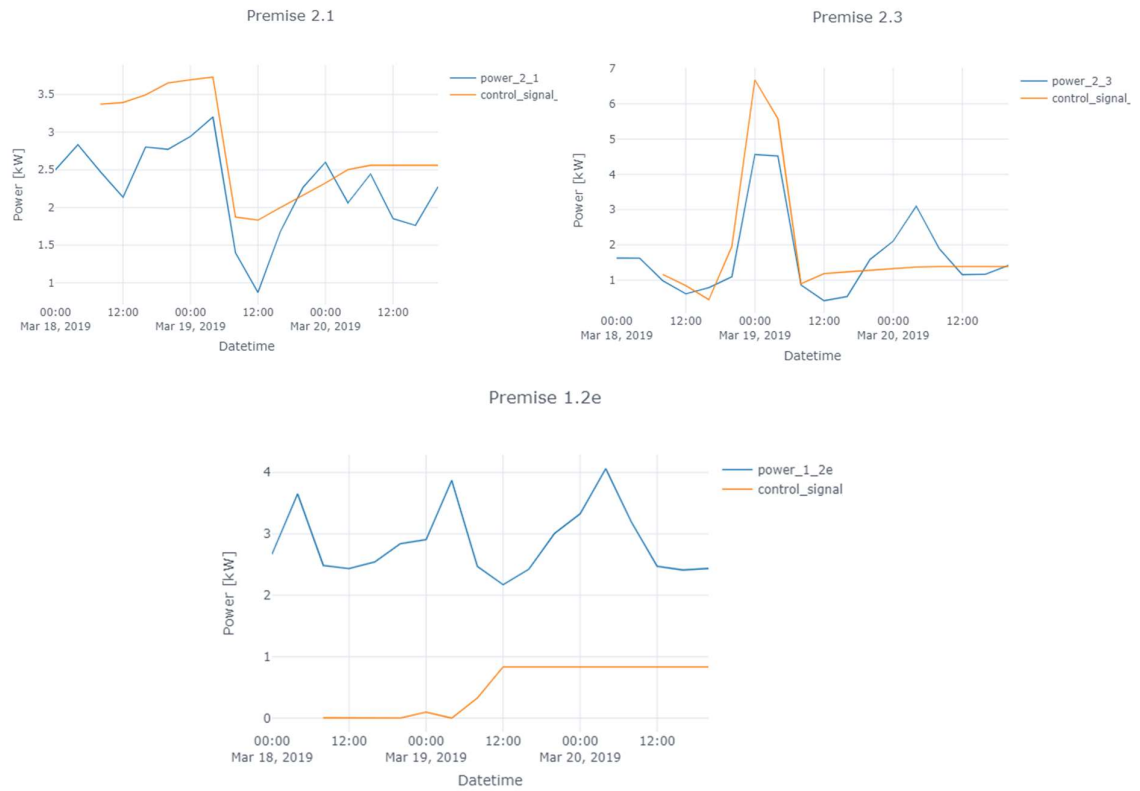


**Figure 30: Comparison building control signal and actual power consumption of the buildings in test Flex\_2 (4-hour average).**

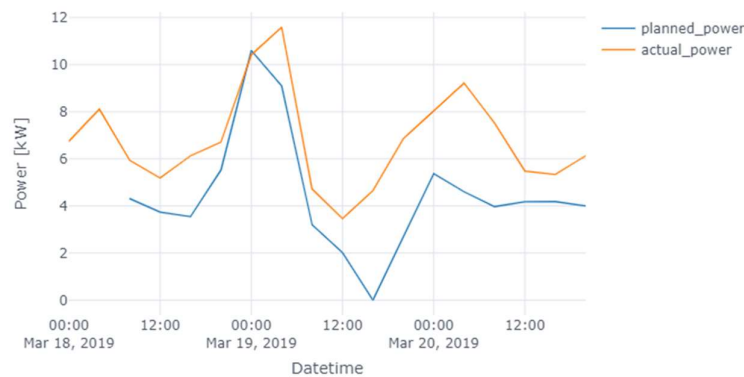


**Figure 31: Comparison of the planned cluster consumption profile and the actual aggregated measured consumption of the cluster in test Flex\_2.**

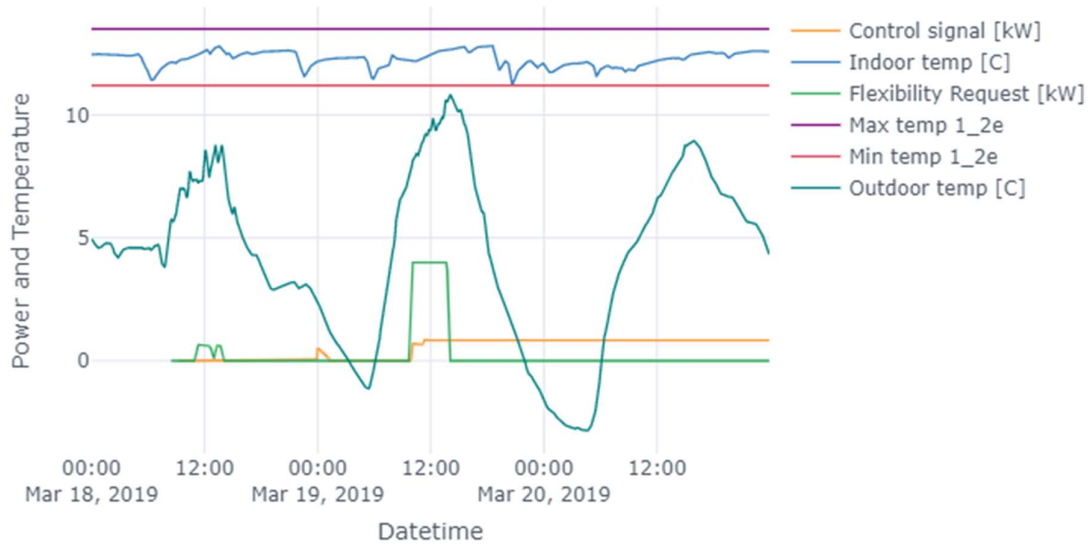


Figure 32: Summary of P1.2 (E) data in Flex\_2 test<sup>9</sup>.

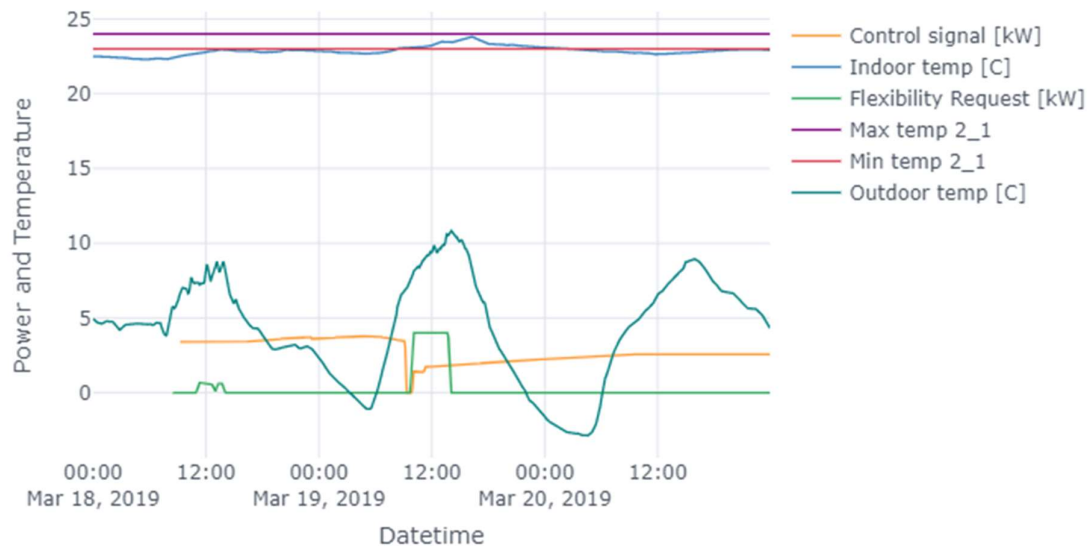
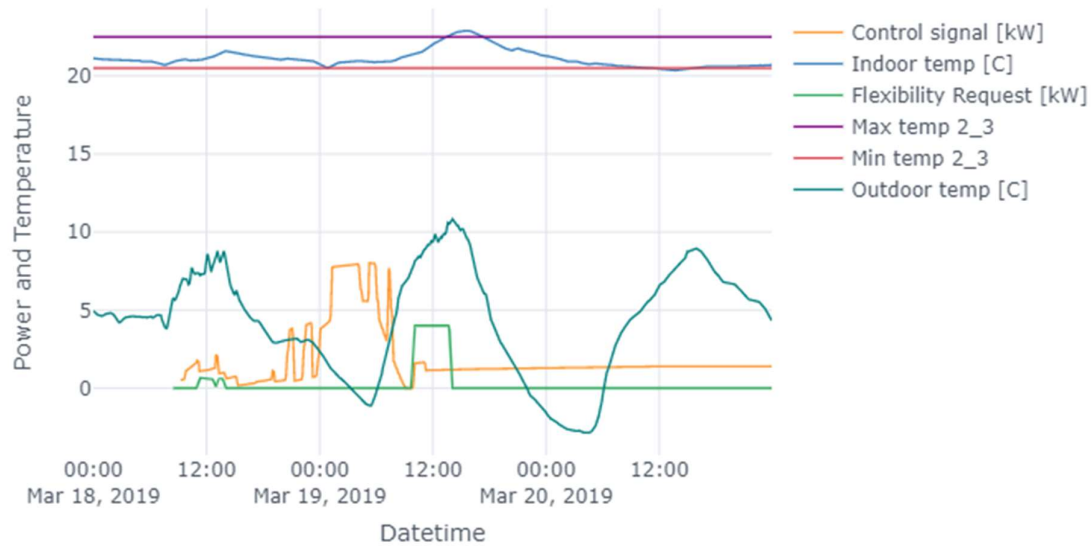


Figure 33: Summary of P2.1 data in Flex\_2 test.

<sup>9</sup> The depicted Flexibility Request in this and the next figures, is the total Flexibility Request for the cluster, which gets disaggregated over the different buildings of the cluster.



**Figure 34: Summary of P2.3 data in Flex\_2 test.**

### 3.2.2.3 Flex\_3 Improved flexibility test

After further analyzing the results of the Flex\_2 test, some further improvements were done to improve the results even more. The results of these modifications were analyzed in the Flex\_3 tests.

As a first improvement, the building models were further calibrated with new data. As a second improvement, the rolling horizon method was adjusted to re-plan after every 90 minutes (instead of 6 hours), which allows to correct for building state – e.g. indoor temperature – errors with this frequency. The flexibility requests are similar to the ones in the Flex\_2 test except the 4-hour flexibility of 4 kW is now requested in the afternoon from 13:00 to 17:00, you can also see in Figure 37 that the flexibility request deviates a little on 2019-03-27 and 2019-03-29.

From Figure 35, we see that both residential Premises 2.1 and Premise 2.3 follow the intended consumption quite well. However, in the industrial Premise 1.2 (East) the planned consumption profile does not match the measured profile. Despite that, the aggregated cluster profile still follows the trend in the planned consumption profile well, as shown in Figure 36.

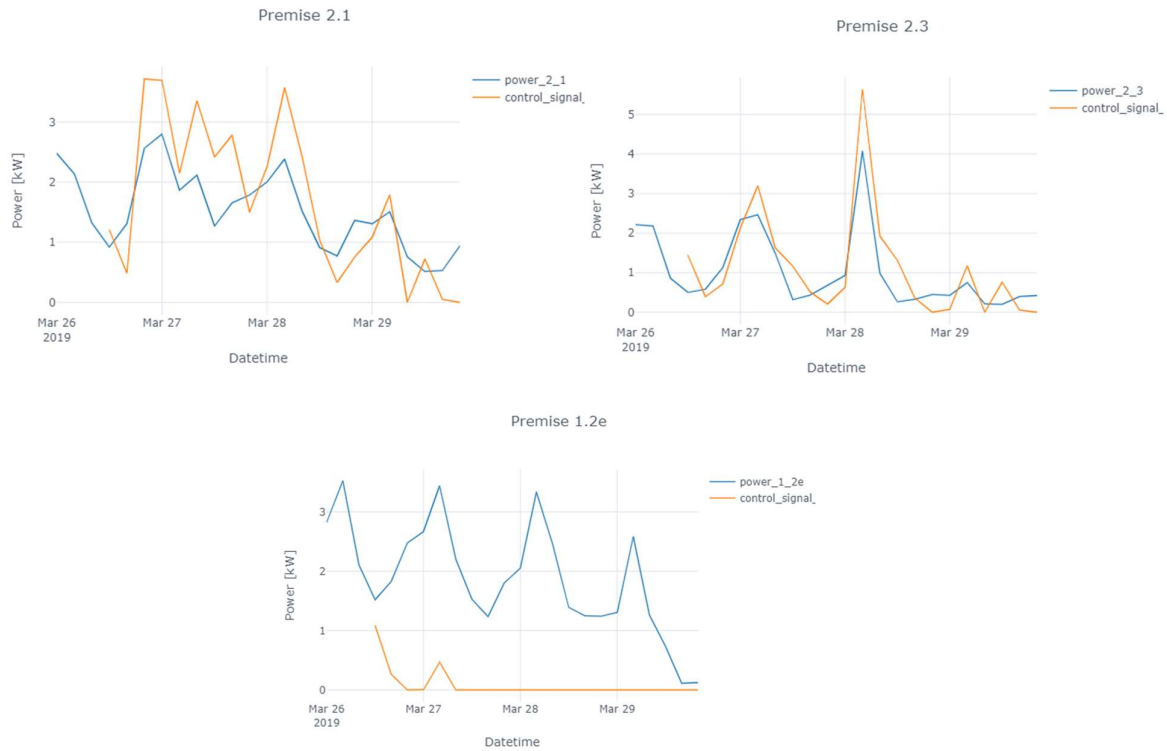


**Figure 35: Comparison building control signal and actual power consumption of the buildings in test Flex\_3 (4-hour average).**

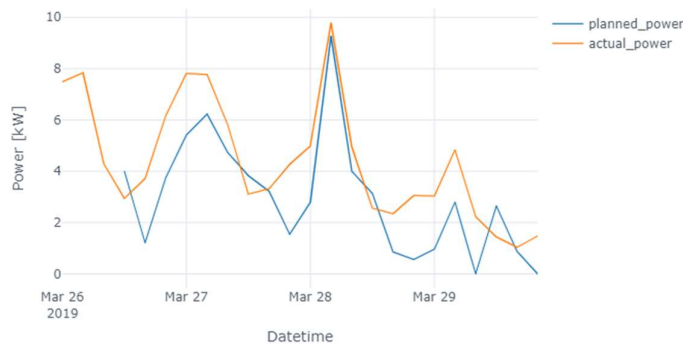


**Figure 36: Comparison of the planned cluster consumption profile and the actual aggregated measured consumption of the cluster in test Flex\_3.**

In Figure 37, Figure 38 and Figure 39, we clearly see how the control signals that were sent to the buildings splits the need for flexibility (by the DSO) between the participating buildings. This is achieved by the ADMM algorithm sending the shadow prices to the buildings. From the orange line Figure 38 and Figure 39 it is apparent that Premise 2.1 and Premise 2.3 both supply around half of the overall flexibility request while Premise 1.2 (East), cfr. Figure 37, is not contributing to the request. These graphs also show that the flexibility requests coincide with high outdoor temperatures, e.g., when there is more solar energy, which are the expected times



for RES curtailment. All graphs show the indoor temperature and their corresponding comfort boundaries. It is seen that these comfort boundaries are respected on most times but exceeded a little during some times. This can be caused by the error in the outdoor temperature forecast or the accuracy of the building model.

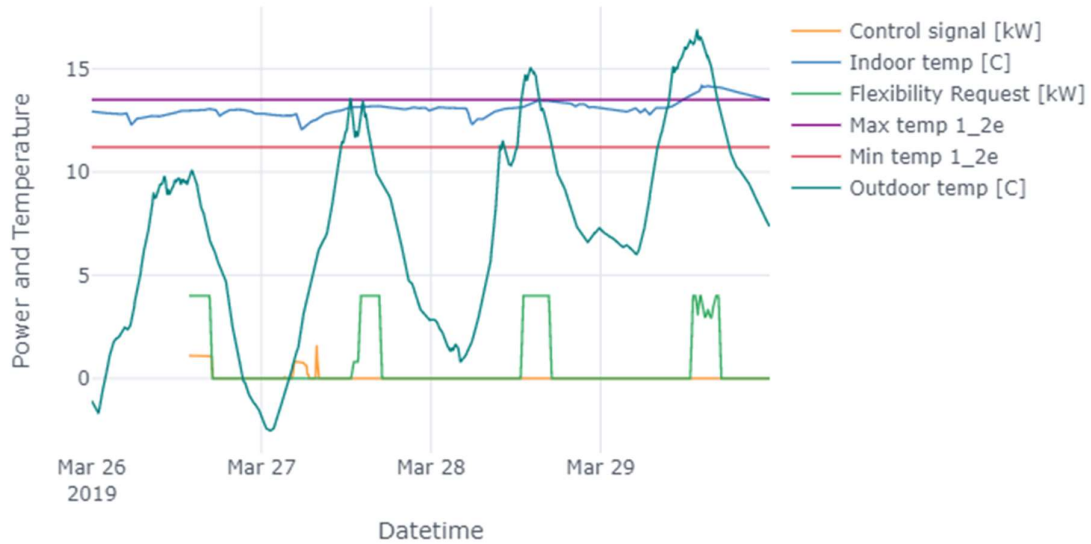


**Figure 37: Summary of P1.2 (E) data in Flex\_3 test.**

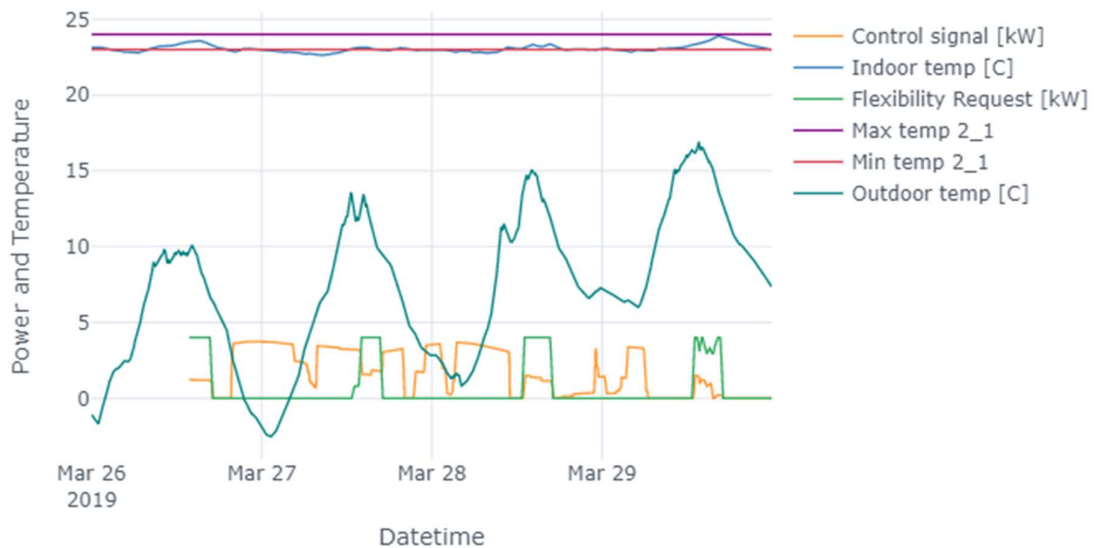


**Figure 38: Summary of P2.1 data in Flex\_3 test.**

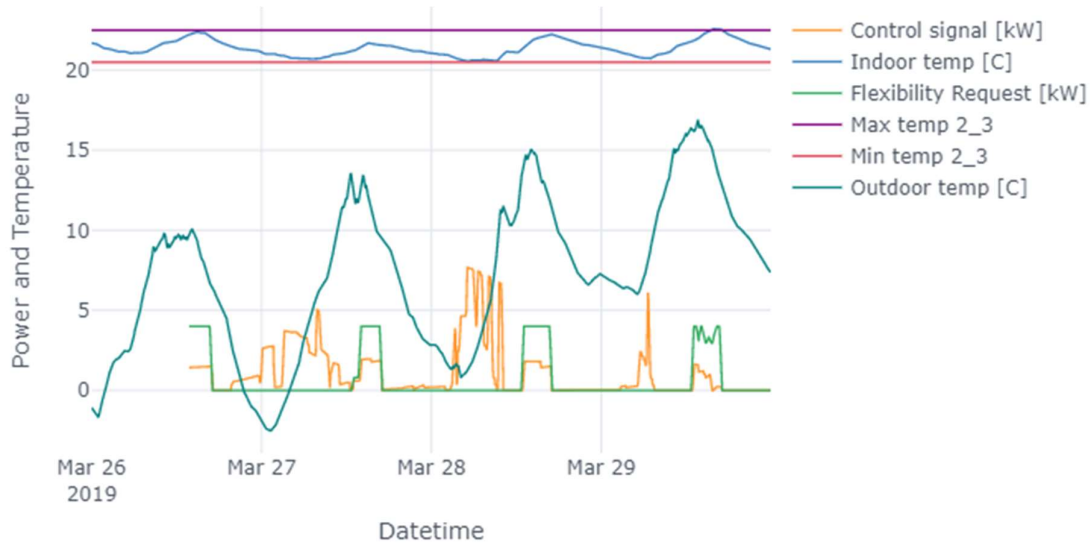


**Figure 39: Summary of P2.3 data in Flex\_3 test.**

In Figure 40, we see that the outdoor temperature override signal (i.e. HP control signal) being applied to the building is in line with the flexibility request that was sent by the DSO. Negative temperature offsets are applied when there is a request to increase consumption of the heat pump, this negative offset makes the heat pump believe that it is colder outside than it really is and therefore it will increase its heating output and its electricity input.



**Figure 40: Building control signal and temperature offset Premise 2.1 in Flex\_3 test.**

As for the other performance indicators, the correlation coefficients of all tests except that of Premise 1.2 (East) showed similar values as No\_Flex. The statistical tests showed that all signal pairs except Premise 1.2 (East) had  $p$  values  $\leq 0.005$ .

The sMAPE values were however higher (between 30-60 %). Premise 1.2 (East) was again with a higher sMAPE. The higher sMAPE values arise from the presence of more values closer to zero), which has the effect that even a lower error in absolute terms leads to a higher relative error which leads to higher percentages. SO comparing sMAPE numbers calculated for different test runs must be done with care.

### 3.2.3 Summary of learnings from VITO integrations tests.

The main learnings and next step actions are summarized below.

With respect to flexibility services that can be offered by heat pumps using the proposed indirect control approach for retrofit situations:

- the determining factor is the Heatpump internal controller, as was concluded as well from the lab experiments of T2.4. These heatpump internal controllers are currently typically developed without flexibility provisioning in mind, meaning that there is no need for them to support the fine granular control and deterministic responses that we are trying to achieve. From T2.4 it was clear that there is a huge difference between different brands and models. In the pilot testing, we were constrained to the heat pumps that were present in the buildings.
- Next to this, also the Heatpump signature model, that is needed to convert a desired consumption profile (i.e. building control signal) into a heatpump control signal (outdoor temperature override signal profile) is important. In these Swedish pilot tests, such a model was constructed from coarse granular (hourly values) historical data, that did not distinguish between space heating cycles and domestic hot water generation cycles. This undoubtedly is a limiting factor for what concerns the accurateness and capabilities of the heatpump signature model. Therefore, in the Dutch Pilot test, such a heatpump signature model was created based on finer granular data (10 minute time resolution), using more information (e.g. return temperature), and using data generated from perturbations (a specific characterisation test cycle) which was possible because there was no risk for comfort impact.
- The combined effect of the above two contributing factors places constraints on the type of flex services that can be offered. For the Swedish pilot buildings, it was clear that the more stringent requirements for balancing services cannot be fulfilled. Curtailment mitigation though, that would require less fine granular and deterministic responses, would be possible though. Especially when taking into account that for such type of services, it is acceptable that the response profile 'embeds' the requested profile, as long as no local grid power constraints are violated. If more demanding flex services are to be offered, one should carefully select a proper heatpump brand and model which has a 'flexible' internal controller. In case that the indirect control paradigm (through outdoor sensor override) is to be used, one should devote sufficient attention in creating the heatpump signature



model. It is clear though that the proposed Direct Control approach is preferred by far.

With respect to the human expert-free building modelling, it was concluded that creating the models (i.e. fitting the model parameters) from historical (un-perturbated) measurements is able to capture the buildings' dynamic thermal behaviour in a 'good enough' manner. The resulting model typically does not capture the fast dynamics, but as long as these are small in absolute terms, this does not have an impact on the envisaged 'safe' (i.e. comfort violation free) flex control. The observed dynamic effects were often caused by unmonitored and uncontrollable internal gains or user behaviour (like opening gates), and it would require other specific forecasting and impact modelling approaches to take them into account: these are envisaged to be addressed in future projects. To increase the robustness of the current models, one could attempt to generate richer training data by applying specific perturbations (test cycles) ... yet it must be recognized that other controllers (at the heat demand side: e.g. thermostats) may counteract the intended effect by blocking heat delivery hence higher indoor temperatures and thereby still limit the 'rich-ness' of the collected data.

In this project and pilot test, the focus was on controlling the heatpump to offer flexibility services, by using an outdoor sensor override control signal to steer the heat pump's heat generation i.e. electricity consumption. In practice though, there is likely as well a – possibly counteracting – controller at the heat demand side (i.e. thermostats) that may block heat delivery and thereby prevent the heat pump's intended electricity consumption. To avoid that this interferes with the envisaged heatpump control strategy, one should know the characteristic of the present thermostat(s), and attempt to control the heatpump in a range where it does not get counter-acted by the thermostat control (i.e. the result of heatpump control actions should not trigger thermostat counteracting measures like blocking heat delivery that avoid a comfort violation that is guarded by the thermostat). In this project, in the spirit of a retrofit expert free solution, we dealt with this complexity by trying to learn the thermostat characteristics by analysing measurements. This was done in a semi-manual (hence not fully expert free manner) but could be embedded in a more automated machine-learning approach in future. Yet a preferred solution would be to be able to rely on IoT connected thermostats, which become increasingly more common, which allows to read out (and possibly control) the thermostat setpoint and setpoint changes.

This pilot highlighted a number of important challenges related to an envisaged expert-free approach for retrofit situations. Existing infrastructures are far from ideal, and often even the most basic information that is required to decide on sensor placements is either wrong, incomplete or missing. Specifically, the absence of zone (apartment level) heat meters and absence of thermostat setpoint information lead to the decision to model the multi-apartment buildings as a single zone (single central heatpump that can be controlled, indoor temperature measurement per



apartment that is averaged into an average indoor temperature). Whereas 'per zone' heat meters are likely to be expensive in near future, IoT thermostats are not, and therefore as a first next step improvement, it is intended to employ multizone modelling by using the thermostat information combined with indoor temperature measurements to create heat delivery disaggregation models.



## 4 Swedish Pilot, TECNALIA building agent services

### 4.1 Model accuracy

#### 4.1.1 Background

The TECNALIA Blackbox model training algorithm takes as input features the outdoor conditions, the indoor current temperatures and the provided thermal energy, and delivers as output the indoor temperature that will be achieved, as well as thermal energy profile required to satisfy it, i.e. the baseline.

During the training phase, k-means is used to create clusters that define the building behaviour taking as reference the indoor comfort constraints, the building usage pattern (energy signature) and the outdoor conditions. The building behaviour is discretized using labelled data as input for K-NN training. The day ahead forecasts are used as input for the trained K-NN model to obtain the 24-hour ahead reference energy consumption.

In practice, the k-means algorithm is very fast, but it may fall in local minima. In order to avoid this behaviour this process has been implemented by means of integrating k-means runs into Monte-Carlo loops following the concept described by the author in **(W.D, Monte Carlo K-Means Clustering)**.

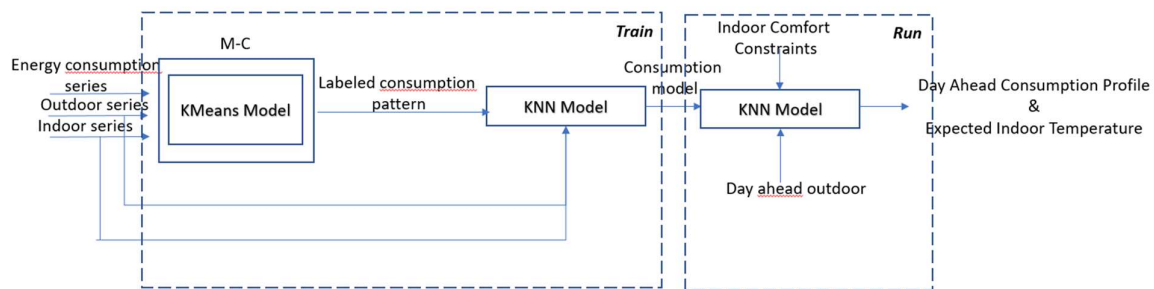


Figure 41: Day ahead consumption and indoor temperature forecast flow.

#### 4.1.2 Analysis

The indoor temperature behaviour is quite extreme, in terms of gap between the warmest and the coolest apartment, in the Premise 2.1 Figure 42. In order to evaluate if this effect is due to the model accuracy or due to some external factors, the historical data for that premise have been analysed too. In Figure 42, it is possible to see how one of the three apartments historically is very much warmer than the rest. The rest of the apartments historically followed more or less parallel indoor temperature profiles, this behaviour has not been disrupted during the pilot period.



**Figure 42: Measured indoor temperatures in the P2.1 apartments.**

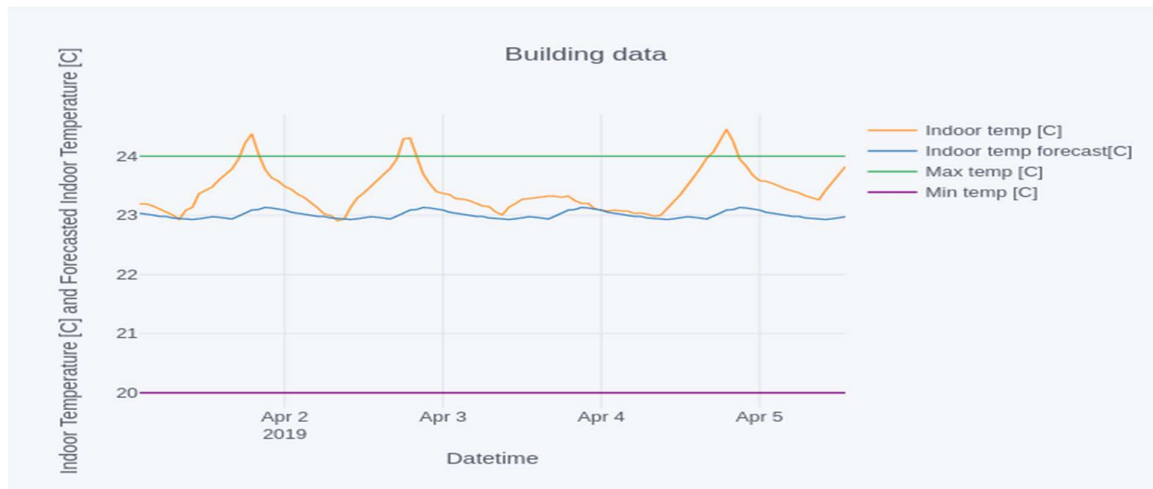


**Figure 43: P2.1 indoor temperatures (average).**

*Note: As there is not real access to thermostats values, the comfort boundaries have been estimated based on the user experience and a restrictive approach to the existing regulation for working areas in the Spain.*

The relevant fact for Premise 2.3 is that indoor temperature follows a quite periodic and regular shape that is suddenly changed for one of the days (below highlighted in red) and recovered later. This behaviour becomes remarkable because it is repeated in two of the apartments (yellow and red lines in Figure 44).



**Figure 44: Measured indoor temperature in the P2.3 apartments.**

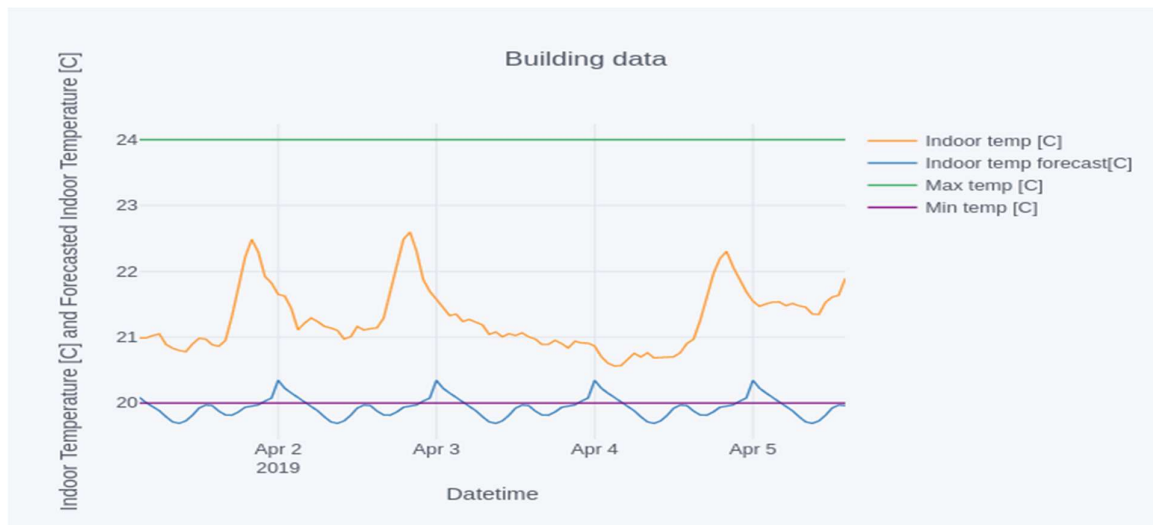


**Figure 45: P2.3 indoor temperatures (average)**

In the figure above it is possible to notice that there is a kind of “gap” that could be considered constant for the whole testing period. In the “Contributing Factors” section will be analyzed the motivations for this behavior.

The statistics to measure the model accuracy are:

- **Pearson correlation:** Evaluates the behaviour of the forecasted and real indoor temperatures, i.e. the scale up and down period are the same for both.

- **SMAPE:** Symmetric Mean Absolute percentage error evaluates the error in % between the forecasted and real indoor temperature.

Pearson Correlation						
Test	1 <sup>ST</sup> day	2 <sup>nd</sup> day	3 <sup>rd</sup> day	4 <sup>th</sup> day	5 <sup>th</sup> day	Average
P2.1	0.51	0.45	0.23	0.42	0.34	0.37
P2.3	0.45	0.27	0.59	0.009	0.30	0.20
SMAPE Value						
Test	1 <sup>ST</sup> day	2 <sup>nd</sup> day	3 <sup>rd</sup> day	4 <sup>th</sup> day	5 <sup>th</sup> day	Average
P2.1	4.45	2.34	1.05	2.1	2.7	2.54
P2.3	7.56	6.4	5.66	5.9	6.78	6.46

**Table 6: Pearson correlation and MAPE values for indoor temperature forecasting in both premises.**

Putting all together, the implemented algorithms and techniques for baseline forecasting and flexibility calculations, after being tested and verified in the integration tests, were applied to Premise 2.1 and Premise 2.3 to evaluate how would they perform in incentive-based flexibility request dynamic scenarios.

Following pricing profiles were used:

- **Baseline Prices:** The baseline pricing profile assumes that there is a fix constant energy cost linked directly to the real consumption. There is not any optimization process applied. The outcome is based in the training done with historical data.
- **Dynamic Positive Prices:** The “only positive” pricing profile is understood as penalties for consumption profile. Economical optimization is applied.
- **Dynamic Positive and Negative Prices:** The mixed prices profile describes periods of the day in which money can be earned and not only saved. Periods of the day with negative pricing represent incomes for the flexibility provider (building owner). Economical optimization is applied.

Figure 46 describes the energy price applied to each of the periods of the day during the testing period. Incent-1 (penalties) and flat-rate profiles assume that there is not additional charging in the periods of the day in which they are applied. On the other hand, Incent-2 shows negative and positive prices. Negative prices mean incoming money from the perspective of the flexibility provider, while positive prices describe money to pay.

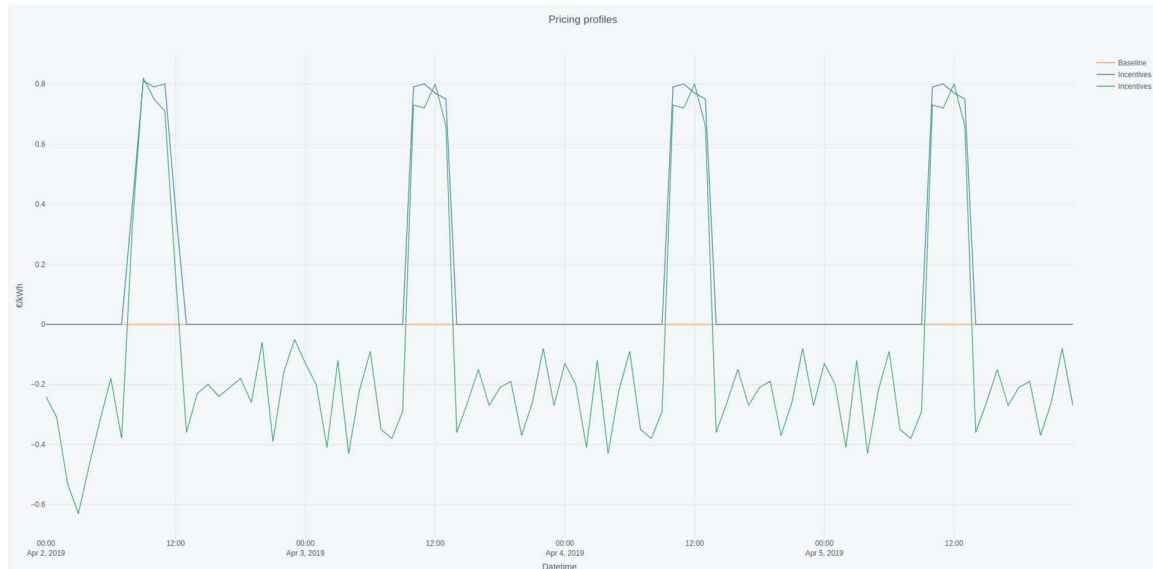


**Figure 46: Incentives/penalties profiles.**

The set of figures below shows power profiles delivered from the pricing schema shown in the previous figure. From the many alternatives to implement the baseline (flat-rate pricing) calculation, the “safe” comfort conditions option has been taken. The “safe” approach considers wide boundaries for the comfort values, so for heating, all the generated thermal power is delivered to the building zones. This is the most common scenario in buildings equipped with water radiators whose manual mechanical valves, usually, are constantly fully open.

*Note: From the Blackbox approach point of view, the assumption above is equivalent to understand that the thermostat or radiator valves remain with the same values during the testing period. Constant values do not have impact in black-box modelling*

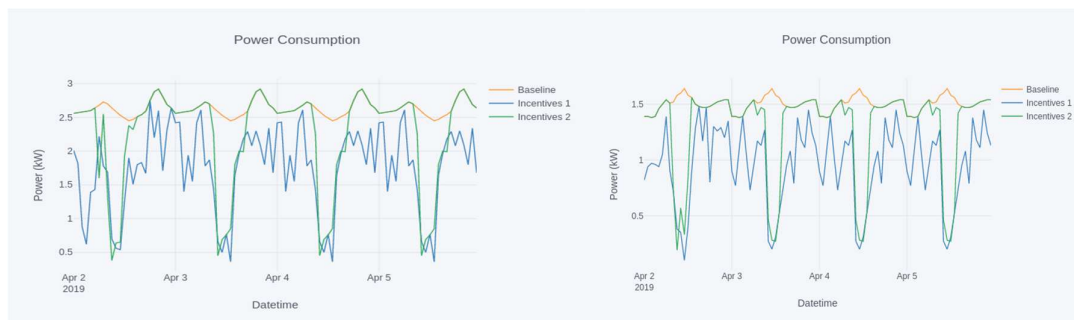


**Figure 47: Building control signal<sup>10</sup> response to incentives for P2.1 (left) and P2.3 (right) compared to the baseline consumption.**

<sup>10</sup> Building control signal is target HP power consumption profile (not to be confused with the HP control signal, which is an outdoor temperature override profile).

The penalties profile (Incent-1) show how the suggested power profile (there are only penalties) tries to minimize the bill to pay and consequently the daily energy consumption. The saving actions take mainly part at periods in which less energy is needed, after midnight and in the periods in which penalties are active. At the other end the negative and positive pricing profile (Incent-2) increases the energy usage in those periods of the day in which the price is negative and decreases at the periods in which is positive. So, the algorithm in this case tries to maximize the income without impacting the calculated baseline consumption.

The following table summarizes the most representative outcomes obtained during the testing period. The energy related rows describe the energy consumption per day in the days in which maximum (Incent-1) and minimum (Incent-2) consumption happened. Additionally, the monetary (€) rows describe the day-based penalties and earnings that happened in the respective days. It is assumed that in Flat-Rate periods no penalties or earning are achieved.

*Note: For the baseline calculation, 0.3 €/kWh was taken as the reference price.*

Premise	P2.1		P2.3	
	Min baseline	Max baseline	Min baseline	Max baseline
<b>Baseline (kWh)</b>	63.15	63.15	65.16	66.63
<b>Incent-1 (kWh)</b>	39.83	42.49	42.21	43.15
<b>Incent-2 (kWh)</b>	53.64	53.75	54.58	56.05
<b>Baseline (€)</b>	18.94	18.94	19.55	19.99
<b>Incent-1 (€)</b>	+ 2.61	+1.78	+1.20	+1.20
<b>Incent-2 (€)</b>	- 11.88	-10.81	-10.45	-11.14

**Table 7: Baseline, consumption and relative billing impact during the testing period. Values for the days in which the minimum and maximum baseline was computed are shown.**

In terms of savings (difference between baseline and the profile in which there are only penalties), measured against baseline, and flexibility (additional consumption from the most energy efficient one) measures between Incent-1 and Incent-2 profiles the following figures are computed.

Premise	P2.1		P2.3	
	Min baseline	Max baseline	Min baseline	Max baseline
<b>Max savings (%kWh)</b> (Baseline-Incent-1) / Baseline	36.7 %	32.2 %	35.3 %	35.3 %
<b>Max flexibility (%kwh)</b> ( (Incent-1-Incent-2)/ Incent-1)	26.0%	21.0%	23.3 %	23.4 %

**Table 8: Summary of result for days in which maximum and minimum baselines were computed.**

The table above describe some figures that are really promising, nevertheless they have to be taken carefully mainly due two reasons:

- The limited testing period that has been used for validation of the results.
- The baseline overestimation that the model could deliver because its training data belonged to cooler days in comparison to those in which it was applied.

It is possible to notice that in both cases, savings and flexibility, it is possible to take huge advantage of penalties/incentives based dynamic management strategies.

- **Strengths and weaknesses:** The robustness of the model is something that it worth to mention. The model was trained with data from the months of February and March, that were mostly cold days. The testing period ran in April included some "warm" days; even though the model was not trained with such higher outdoor temperatures, it was still able to predict the indoor temperature for such higher outdoor temperatures in a good manner
- **Contributing factors:**
  - **Quality of the heat pump signature model for indirect control:** See chapter 2.1.1
  - **Quality of the building thermal model:** The accuracy of the thermal model can be improved by adjusting the training methodology. For the pilot testing the training was done with data almost during the winter period, there has not been any seasonal training nor continuous training approach implement. Any of the options would have had positive impact. The accuracy of the building thermal model has shown in average approximately an 40% for Premise 2.1 and 20% for Premise 2.3 of correlation between the forecasted and real indoor temperatures. Regarding to the MAPE values between 2% and 6% are obtained. Being the SMAPE acceptable good but the correlation



indicates that there can be a shift of the forecasted and measured values that impacts in the correlation but not in big way in the deviation.

- **Quality of exogenous parameters:** The accuracy of the most significant exogenous variable is analysed in chapter 4.2
- **Suggested improvements:** Improvements in terms of addition of thermal sensors, as explained in chapter 4.2 would help to implement more accurate models.

## 4.2 Demand profile following capabilities

### 4.2.1 Background

The demand profile following capabilities testing validates how the building control signal (= proposed consumption profile) generated by the Shapers is followed by the pilot consumption profile. The implemented model based on Black-box numerical models could deliver as outcome, spiky or saw-tooth profiles, not convenient for HP control. In order to avoid that, Savitzky-Golay filter has been used to smoothen the proposed building control signal (consumption profile).

Savitzky-Golay filter is very common in signal processing problems for the purpose of smoothening the data, that is, to increase the precision of the data without distorting the signal tendency.

### 4.2.2 Analysis

Once all the integration tests were passed, testing phase was scheduled for the first week of April. For some technical reasons, the first of the testing days there was not applied effective control signal to any of the two premises. Nevertheless, the day has been kept as part of the pilot testing phase.

The data obtained during the testing period for each of the premises shows some relevant and interesting facts.

- Proposed consumption higher than real consumption: Regarding to the proposed consumption profile (yellow line) it is interesting to point, that it is sometimes time higher than the effective power consumption. This behaviour is shown mainly in Premise 2.1 and leads to think that the reason for that something that impacts in both models, inaccuracy in the HP management, inaccuracy in input data or bias of the modelling approach. From the other hand, as this behaviour is not present in Premise 2.3 shows that the modelling approach is not intrinsically biased to produce higher consumption profiles than required.
- Outdoor temperature: Both pilot sites were located in the city of Karlshamn, so it is reasonable to think that they were under the same outdoor conditions. Comfort boundaries: For the same building modelling approach and optimization approach, we observe that for P2.1 our optimization leads to a



very high indoor T (around the max T of 25 degrees), whereas for P2.3 it is more as expected (i.e. around 21 degrees and more central to the comfort boundaries). In this context comparing to the historical indoor temperature series (Figures 39 and 41) the optimization process did not have negative impact in the indoor comfort conditions.

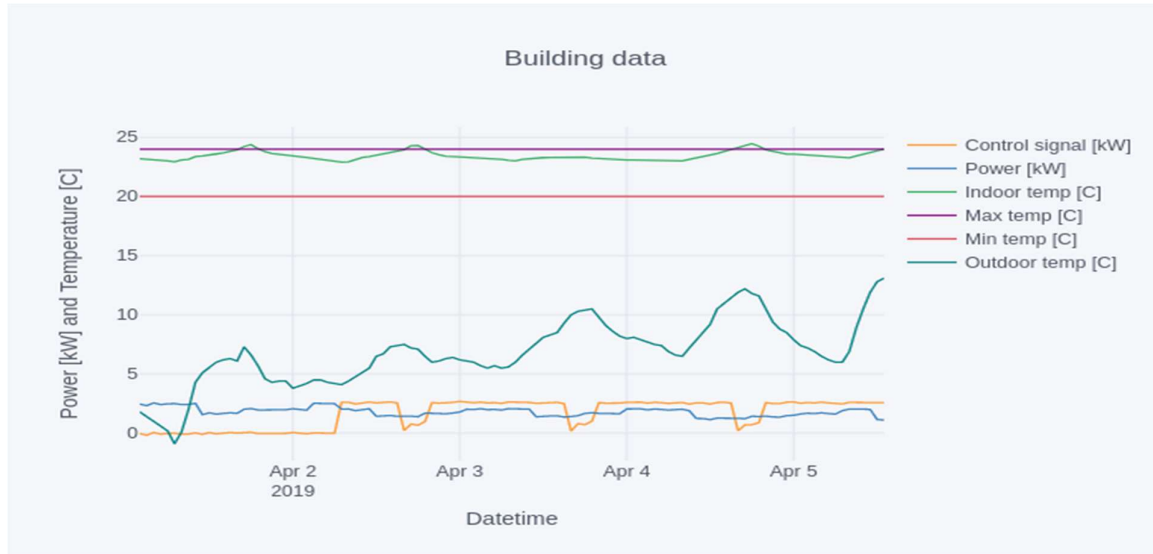


Figure 48: P2.1 energy profiling.

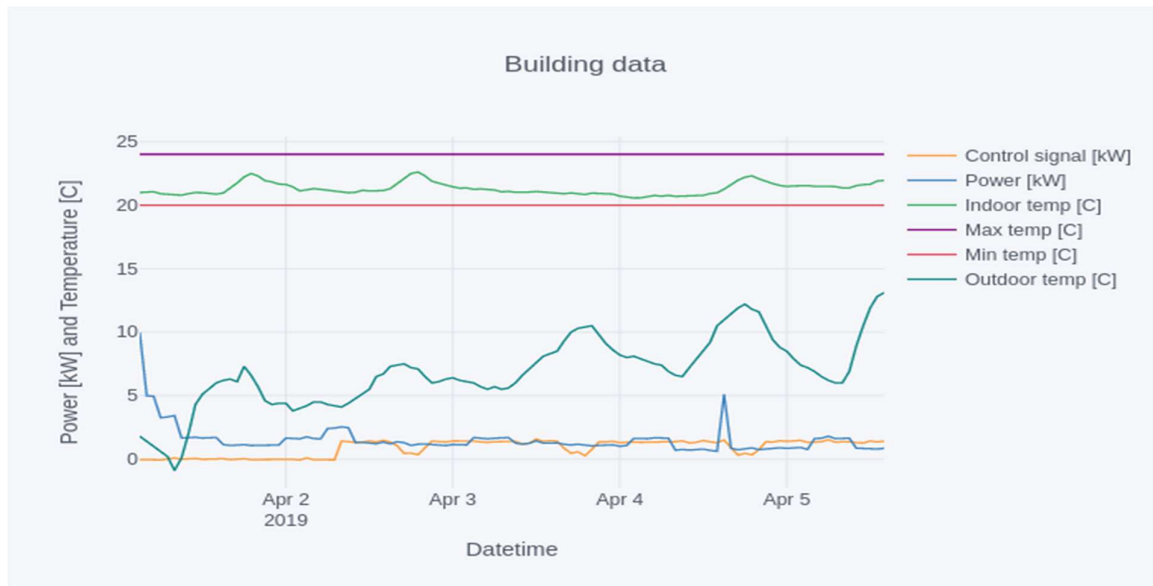


Figure 49: P2.3 energy profiling.

The statistics to measure the accuracy of the control signal are:

- **Pearson correlation:** Evaluates the behaviour of the planned consumption profile (i.e. building control signal) in comparison to the real power, i.e. the scale up and down period are the same for both.
- **SMAPE:** Symmetric Mean Absolute percentage error. In order to avoid undefined values for 2019-04-01, the building control signal (= planned consumption profile) has been taken as reference.

**Pearson Correlation**

Test	1 <sup>ST</sup> day	2 <sup>nd</sup> day	3 <sup>rd</sup> day	4 <sup>th</sup> day	5 <sup>th</sup> day	Average
<b>P2.1</b>	nan	0.48	0.36	0.35	0.005	0.38
<b>P2.3</b>	nan	0.37	0.22	0.31	0.30	0.32

**SMAPE Value**

Test	1 <sup>ST</sup> day	2 <sup>nd</sup> day	3 <sup>rd</sup> day	4 <sup>th</sup> day	5 <sup>th</sup> day	Average
<b>P2.1</b>	>100	70.92	45.3	49.23	41.64	40.01
<b>P2.3</b>	>100	60.55	27.90	44.6	36.67	35.55

**Table 9: Pearson correlation and SMAPE for the delivered consumption profile and the real one**

*Note: nan and >100% values are due to the 0 value of the applied control signal.*

- **Strengths and weaknesses:** The robustness of the generated control signal is something that is worth to mention. Consumption profiles that present erratic behaviour, even in a few known cases, wouldn't be assumable for HVAC systems management. Consumption profiles that vary significantly in short periods of time may deliver, unpredictable behaviour of the HP and consequently building owners discomfort. The identified main weakness is the gap that in some of the periods of the day shows the control signal in comparison with the delivered power.
- **Contributing factors:**
  - Brand and model type of the heatpump (internal controller characteristics): See chapter 2.1.2 for HP signature and capability details.
  - Thermostat or other unknown control equipment: The presence of additional control equipment that may impact in the overall modelling and optimization process is not relevant as far as it is kept in constant value during the pilot phase. The black-box modelling approach is not affected by those values that even being unknown present constant values.
  - **Quality of the heat pump signature model for indirect control:** See section 3.1.1.



- **Quality of the building thermal model:** The impact of the quality of the thermal model will be explained in the next chapter
- **Quality of exogenous parameters:** Inaccuracies on the deployed sensor or bad commissioning has direct impact on the outcome of the model and consequently in the generated control signal. In the same context deviations in the weather forecast may cause significant deviations in the final outcome.

The following chart describes the weather forecast used to feed the models and the outdoor values collected by the pilot monitoring platform and stored in NODA-s servers.

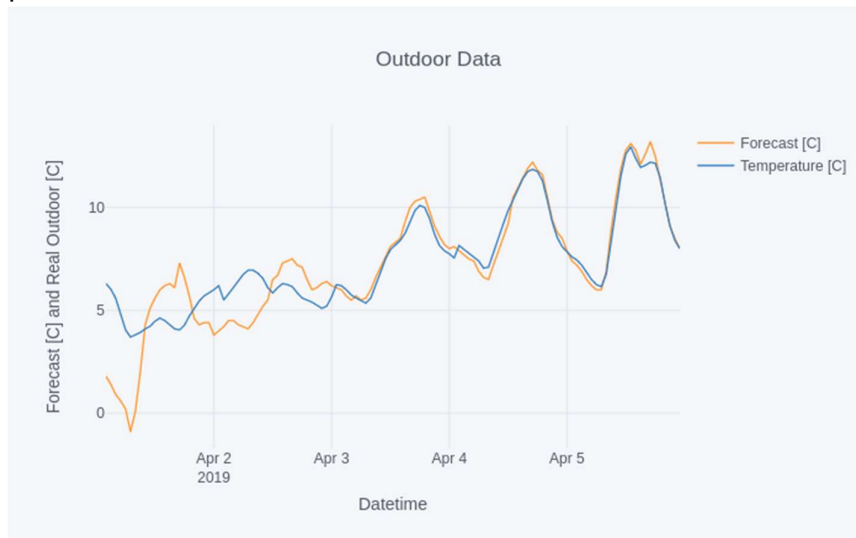


**Figure 50: Forecasted and measured outdoor temperature.**

From the figure (Figure 50) it is possible to conclude that the weather forecast and the real temperature were quite similar for some of the piloting days but not always as it could be expected.

- **Suggested improvements:** The installation of thermal meters to measure produced real thermal power and some digital IO that indicates the status of the HP could enrich the training data set and help to produce more accurate models that finally would deliver more realistic control signals.

## 5 Impact Analysis by extrapolation of results

We evaluate the joint ability, i.e., the ability of central ECOVAT-like deployments together with distributed building heatpump deployments, to reduce injection peaks of intermittent RES-E by shifting P2H consumption to (forecasted) injection peaks.

By explicitly shifting P2H consumption to (forecasted) times of peak injection, there will be less of such P2H consumption at times of low injection (assuming the overall P2H consumption is not impacted by the shifting). As the combined effect of this, there will be a more even spread of injection (i.e. smaller difference between peaks and valleys).

The amount of intermittent RES-E that can be captured with the FHP P2H solution can be estimated by repeatedly solving an optimisation problem against historical data (Day Ahead, Intraday, Current), subject to experimentally determined flexibility capability of P2H solutions, and some assumptions on ECOVAT market share, and then compare the distribution of RES-E injections with and without the actively controlled P2H consumption. This is being defined as a valuable KPI to assess the potential impact.

### 5.1 Scenario

The calculation of this 'injection' distribution KPI to quantify the potential impact of the FHP proposed actively controlled P2H solutions, was structured as an optimization problem consisting of two nested parts::

- optimisation of the Day Ahead intermittent RES-E peak capturing subject to building flexibility, as demonstrated in T4.4, and
- optimisation of the capturing of the deviation of Intraday intermittent RES-E from Day Ahead intermittent RES-E subject to some standard deviations of ECOVAT flexibility, as demonstrated in T4.3,

where the standard deviations of ECOVAT flexibility refer to the variation of the deviation of Intraday intermittent RES-E from Day Ahead intermittent RES-E, and serves to model the market share of the ECOVAT solution.

The deviation of Current intermittent RES-E from Intraday intermittent RES-E is then added to the solution to model the shortcomings of the present-day electricity market, resulting in a conservative estimate. In greater detail,

$$\begin{aligned}
 x^* &= \min_x \|a + x\|_2^2 \\
 a^* &= a + x^* \\
 y^* &= \min_y \|a^* + (b - a) + y\|_2^2 \\
 b^* &= a^* + (b - a) + y^* \\
 c^* &= b^* + (c - b),
 \end{aligned}$$

where  $a$  is the Day Ahead vector,  $b$  is the Intraday vector,  $c$  is the Current vector,  $x$  is the correction of the Day Ahead vector,  $y$  is the correction to the Intraday vector,  $x$  and  $y$  are subject to the above-mentioned constraints in the form of linear equalities, and asterisks indicate the corresponding optimal values.

### 5.1.1 Flexibility provided by buildings

We shall use convex programming and to this end express the available building flexibility by linear inequalities bounding the offset  $\Delta P$  [kW] in electricity demand,

$$\Delta P \in \Delta_{[\min, \max]} P = [\Delta_{\min} P, \Delta_{\max} P]$$

$$\Delta Q \in \Delta_{[\min, \max]} Q = [\Delta_{\min} Q, \Delta_{\max} Q]$$

where  $\Delta Q$  [kWh/h] is the mean value of  $\Delta P$  over the last 24 hours.

Given a building model subject to constraints on the indoor climate, the above constraints can be estimated through simulation, with the constraints on  $\Delta P$  bounding short-term deviations of the indoor climate from the preferred indoor climate, and the constraints on  $\Delta Q$  bounding long-term deviations of the indoor climate from the preferred indoor climate.

The metrics  $\Delta_{[\min, \max]} P$ ,  $\Delta_{[\min, \max]} Q$ , and the installations mean electricity demand  $P_{\text{mean}}$  [kW] over a period of interest, in our case, 2018-10-01/2019-04-01, can be used to compute two interval-valued key performance indicators,

$$\Delta_{[\min, \max]} P / P_{\text{mean}}$$

$$\Delta_{[\min, \max]} Q / P_{\text{mean}}$$

Here,  $P_{\text{mean}}$  serves to measure the size of the installation, and the divisions by  $P_{\text{mean}}$  give values that can be used to estimate how the available flexibility independent of the size of the grid.

In Task 4.4, the buildings were subject to safety constraints on the form  $\Delta_{[\min, \max]} P = [-\Delta_{\max} P, \Delta_{\max} P]$  and  $\Delta_{[\min, \max]} Q = \Delta_{[\min, \max]} P / 2$ , with no adverse effects to the indoor climate despite exercising a range of extreme control signals. Consequently, it is reasonable to use the safety constraints as proxy for the building flexibility, with the advantage that it can be used together with historical data to estimate the distribution of  $\Delta_{\max} P / P_{\text{mean}}$  for a realistic building stock.

An estimate based on 70 buildings in Karlshamn, Sweden, gives the roughly normal distribution of Figure 51, with mean 17.2 % and standard deviation 3.7 %.

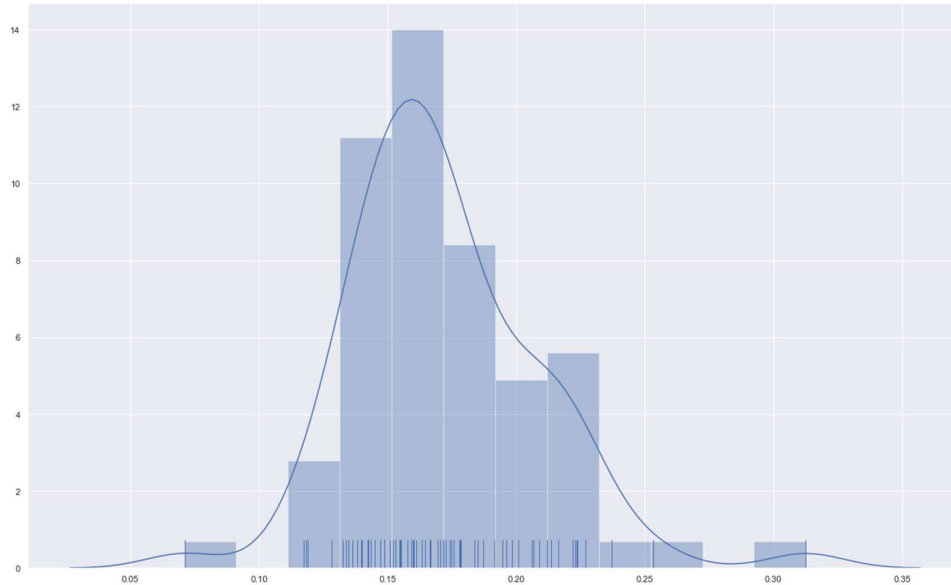


**Figure 51: Distribution of  $\Delta_{\max} P/P_{\text{mean}}$  based on 70 buildings in Karlshamn, Sweden.**

### 5.1.2 Flexibility provided by ECOVATs

The proposed scenario dimensions the ECOVAT against the intraday market, with the intraday and imbalance markets expected to be economically more advantageous than the day-ahead market, and hence a better focus for the early commercialisation of the ECOVAT solution. This assumption makes it possible to quantify the ECOVAT market share in terms of standard deviations (SD) of the intraday market as in Table 10. That is,  $\pm 0$  SD amounting to a negligible share, and  $\pm 3$  SD amounting to the capacity to absorb 99.7 % of the intraday market.

SD	ECOVAT share of the Intraday market <sup>11</sup>
$\pm 0$	0.0 %
$\pm 1$	68.3 %
$\pm 2$	95.5 %
$\pm 3$	99.7 %

**Table 10: ECOVAT market share in terms of standard deviations of the intraday market.**

### 5.2 Data

We evaluate the FHP solution across several scenarios based on hourly data from the European Network of Transmission System Operators for Electricity (ENTSO-E) Transparency Platform<sup>12</sup>. The data pertains to country of Belgium and the period

<sup>11</sup> The analysis is done relative to an Intraday market, such that the methodology could be applied at a local context, or a country level context, or the complete EU context.

<sup>12</sup> <https://transparency.entsoe.eu>

2018-10-01/2019-04-01 of the two demonstrations, and covers Solar (Day Ahead, Intraday, Current = Intraday), Wind Offshore (Day Ahead, Intraday, Current), and Wind Onshore (Day Ahead, Intraday, Current), see Figure 52, Figure 53 and Figure 54.

Note that the choice of country is not expected to affect the evaluation, whose purpose is to evaluate the solution against the shape of the natural variation of intermittent RES-E rather than against national regulations.

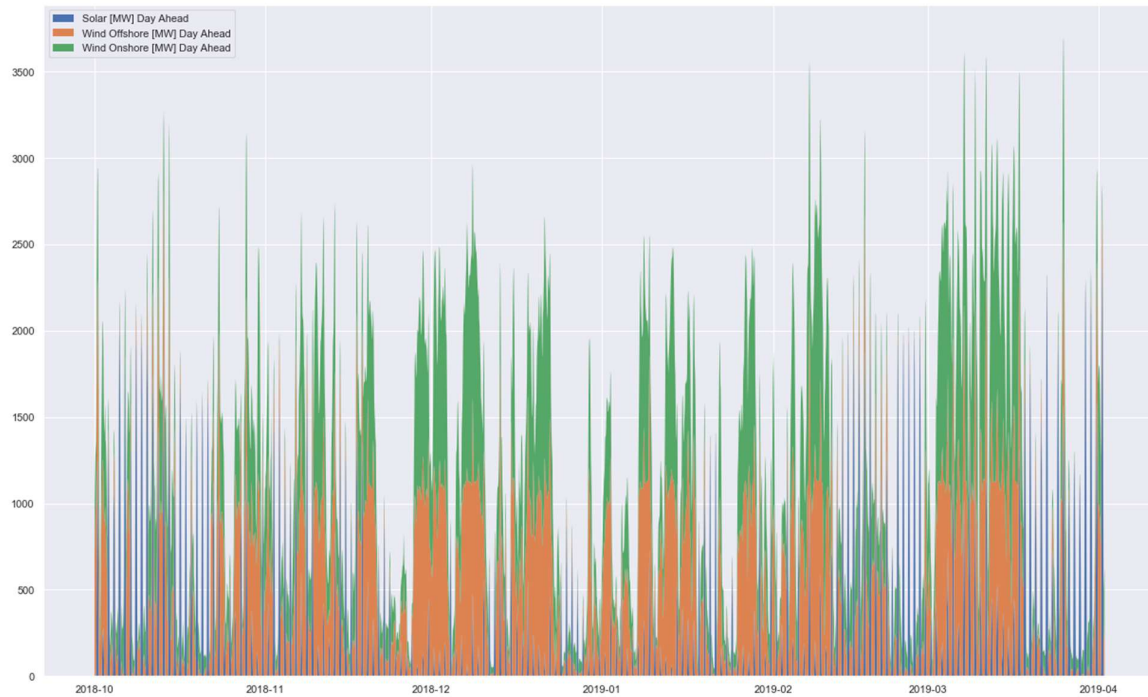


**Figure 52: Belgium: Intermittent RES-E [MW] Day Ahead.**

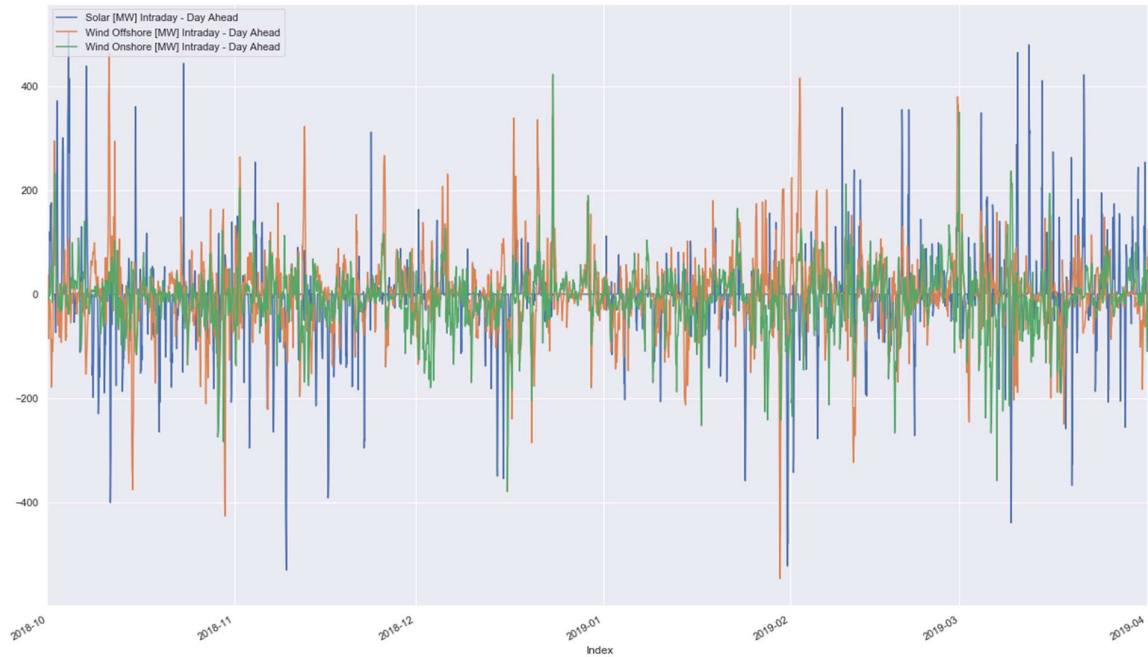


**Figure 53: Belgium: Intermittent RES-E [MW] Intraday - Day Ahead.**

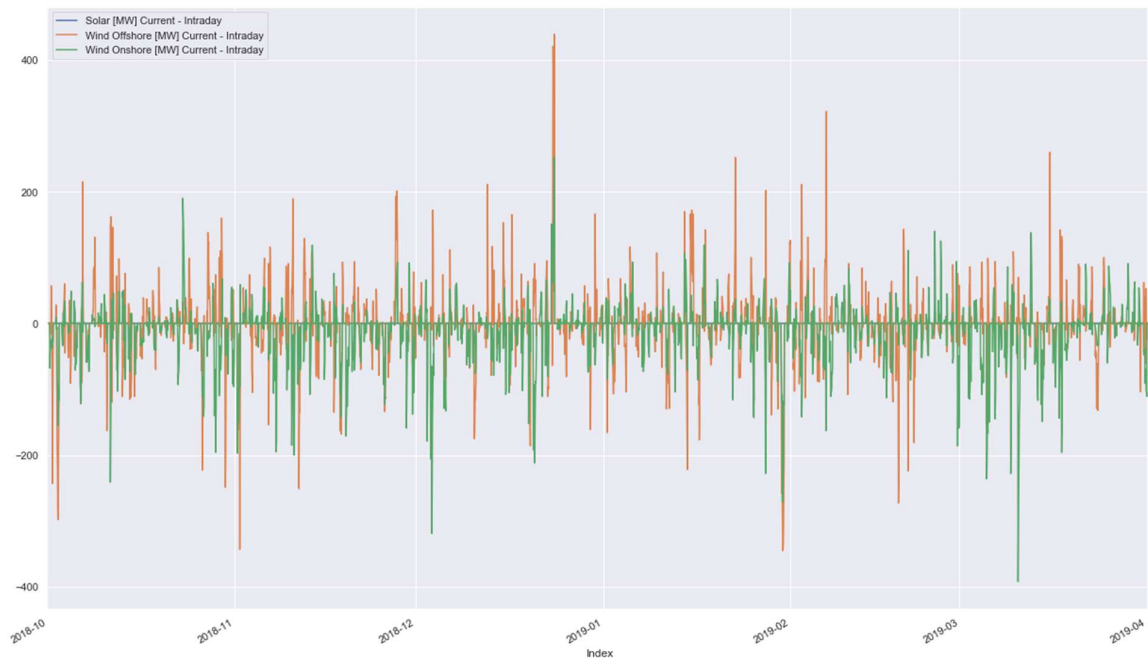


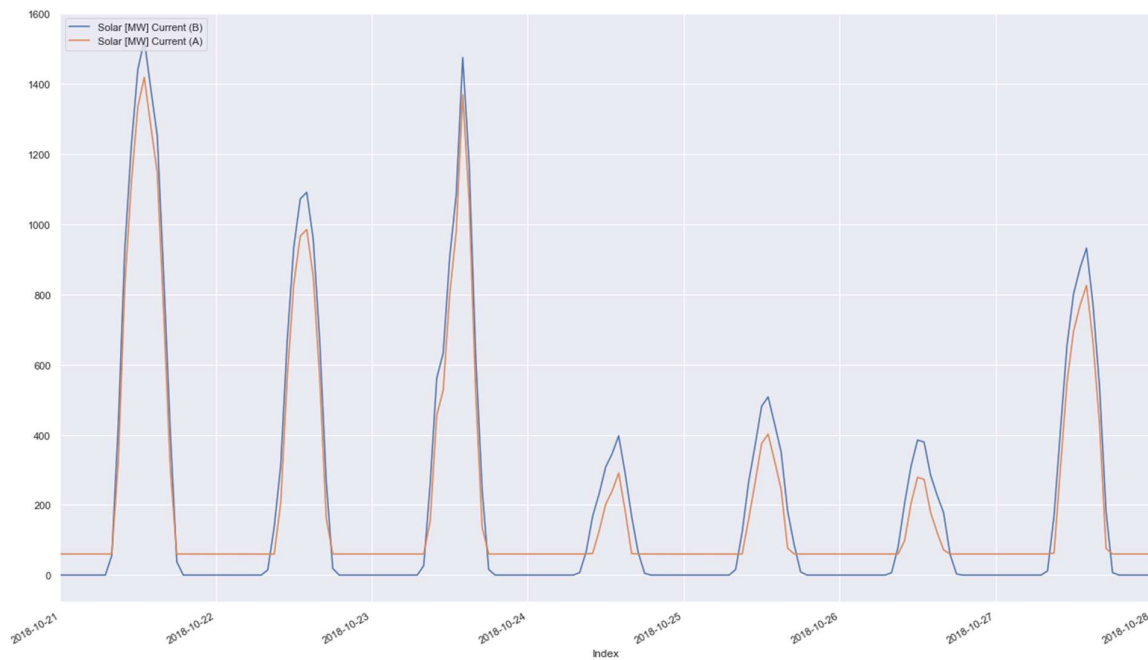
**Figure 54: Belgium: Intermittent RES-E [MW] Current – Intraday.**

In addition to the above implied scenarios of different types of intermittent RES-E, it is also necessary to decide on how to model a local grid. As for the latter, note that due to the aggregated nature of the national data, it will be less volatile than local data. And while unfortunate for the purpose of demonstrating the capabilities

of the solution, it will consequently provide a more conservative estimate than local data of the natural variation of intermittent RES-E in a local grid, and hence a more conservative estimate of the mean capabilities of the solution.

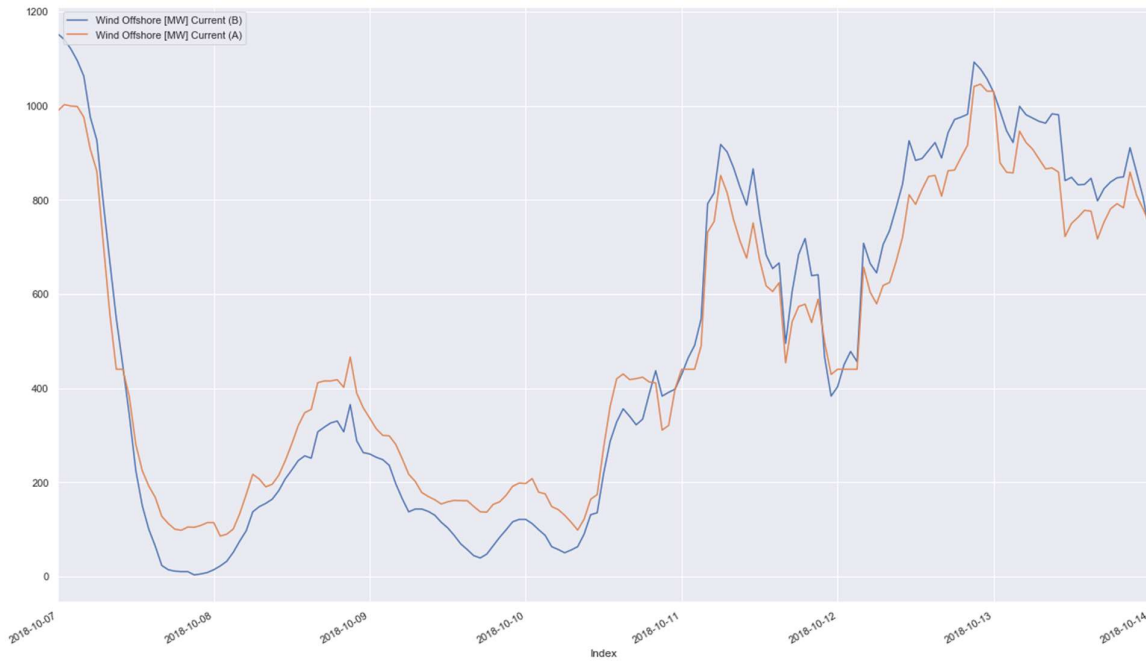
### 5.3 Results

Figure 55, Figure 56, Figure 57 and Figure 58 demonstrate how P2H demand can be shifted with the FHP solution for an ECOVAT market share of  $\pm 1$  SD, effectively making the supply of intermittent RES-E appear more evenly distributed in time by shaving (reducing) the peaks while at the same time increasing the valleys.



**Figure 55: Belgium: Solar [MW] Current (Before, After  $\pm 1$  SD).<sup>13</sup>**

<sup>13</sup> In this and the following figures, B refers to Before i.e. without applying active steering of P2H flex, whereas A = After refers to applying the active steering of such P2H flex.



**Figure 56: Belgium: Wind Offshore [MW] Current (Before, After  $\pm 1$  SD).**



**Figure 57: Belgium: Wind Onshore [MW] Current (Before, After  $\pm 1$  SD).**

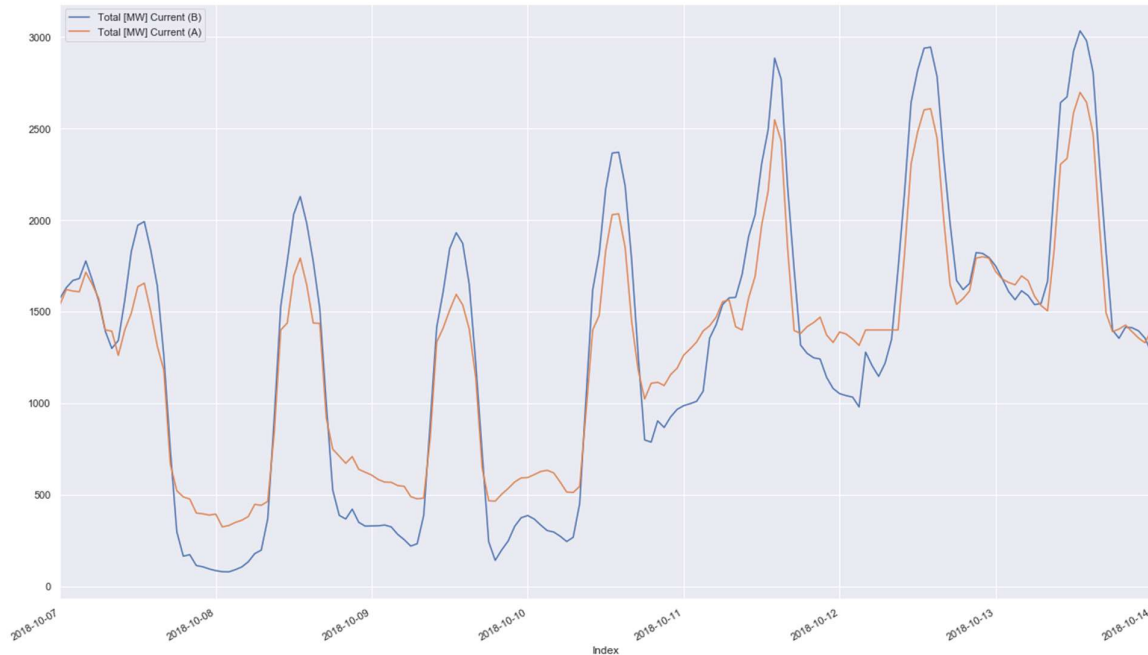


**Figure 58: Belgium: Total [MW] Current (Before, After  $\pm 1$  SD).**

Figure 59, Figure 60, Figure 61 and Figure 62 show the distribution of current intermittent RES-E before and after the FHP solution for an ECOVAT market share of  $\pm 0$  SD,  $\pm 1$  SD,  $\pm 2$  SD and  $\pm 3$  SD. The distributions for Solar and Wind Onshore are roughly exponential, while the distributions for Wind Offshore displays a bimodal pattern. The bimodal pattern was unexpected, and it is unclear whether the Wind Offshore data can be considered representative. Nevertheless, it is evident from the concentration of the distributions that the FHP solution serves to evening out the apparent electricity supply.

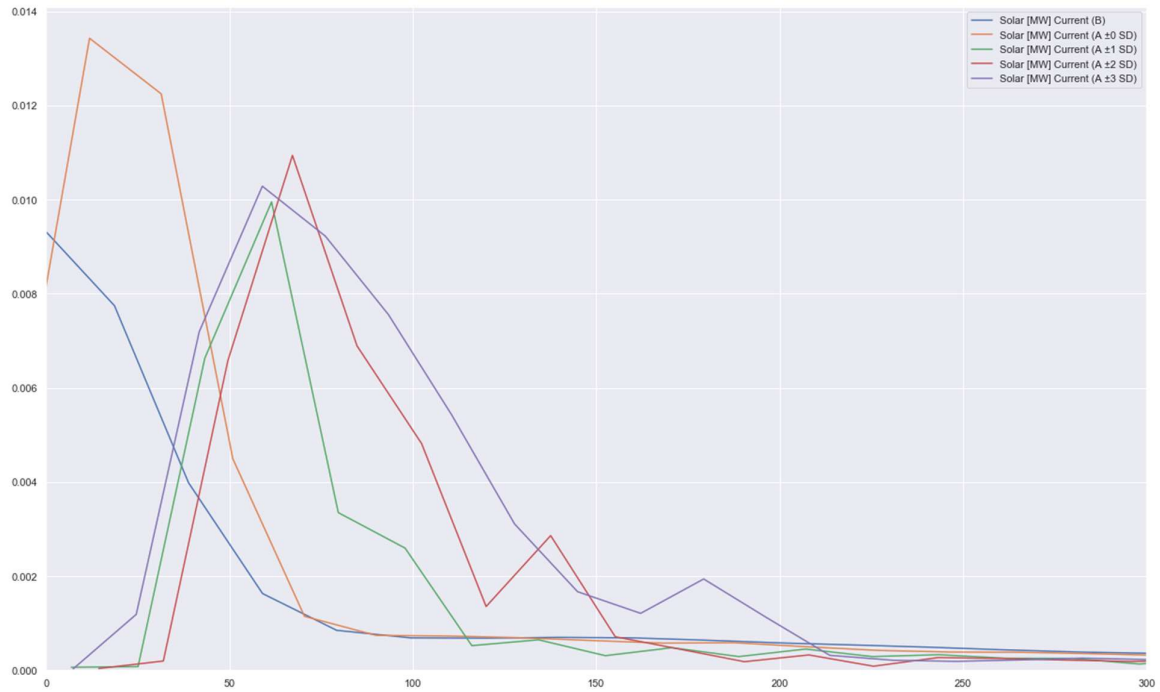


**Figure 59: Belgium: Solar [MW] Current KDE (Before, After  $\pm n$  SD).**

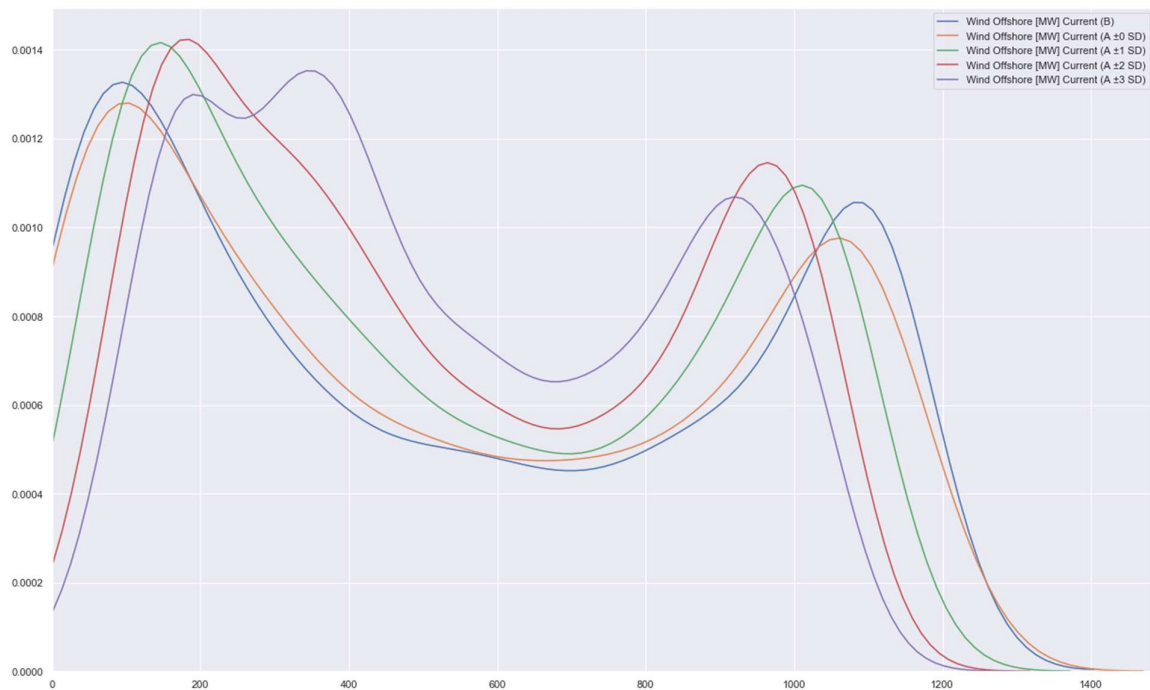


**Figure 60: Belgium: Wind Offshore [MW] Current KDE (Before, After  $\pm n$  SD).**

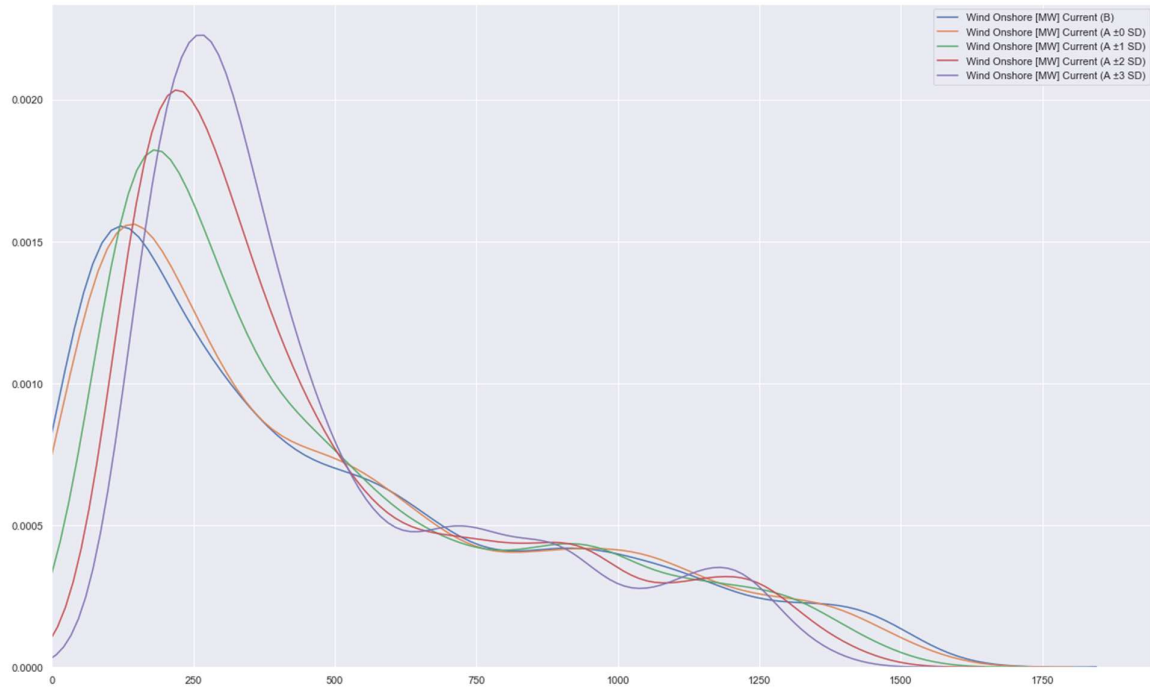


**Figure 61: Belgium: Wind Onshore [MW] Current KDE (Before, After  $\pm n$  SD).**

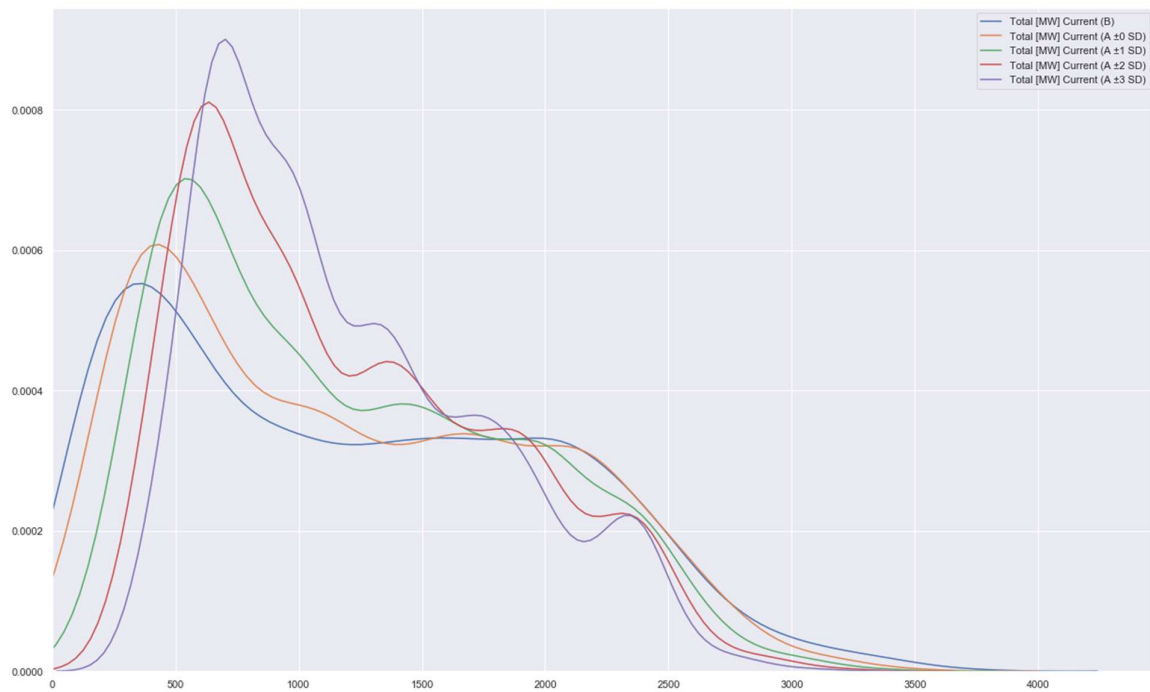


**Figure 62: Belgium: Total [MW] Current KDE (Before, After  $\pm n$  SD).**

Compiling the results across the different scenarios, and comparing standard deviation of the distributions before and after the FHP solution, we arrive at Table 11 below.

<b>Before/After</b>	<b>±0 SD</b>	<b>±1 SD</b>	<b>±2 SD</b>	<b>±3 SD</b>
Solar	14.2 %	24.2 %	34.7 %	45.8 %
Wind Offshore	1.7 %	13.5 %	25.6 %	37.1 %
Wind Onshore	1.7 %	10.7 %	19.6 %	28.0 %
Total	5.9 %	18.0 %	30.6 %	43.2 %

**Table 11: Comparison of distributions: SD(Before) / SD(After) – 1.**

The table shows that while the building solution performs well for Solar, it performs less well for Wind, in contrast with the ECOVAT solution, which performs well across the board. This can be understood from the distribution of the different energy sources across time, cf. Figure 52, and how they interact with the available flexibility. On the one hand, building flexibility can be used to shift electricity demand across hours, but not across weeks. Consequently, while it is well suited to address the regular day/night cycle of solar power, it is less well suited to address the irregular but persistent nature of wind power. On the other hand, ECOVAT flexibility performs more evenly across different energy sources, and while here dimensioned to trade on the intraday market, it nevertheless serves to shift electricity demand across weeks.

Integrating the Kernel Density Estimates of Figure 59 gives the Cumulative Distribution Functions of Figure 60, closely related to the concept of Load Distribution Curves commonly used to analyse energy data. The difference is only that of a coordinate change from probability  $p$  to the probability  $1 - p$  of the horizontal axis, accompanied by a corresponding change of interpretation. The graphs give an idea of how the FHP solution can be used to avoid curtailment. For example, consider a situation where it is necessary to curtail power above 2000 MW. Without the FHP solution, this would occur with a probability of  $1 - 0.78 = 0.22$ , i.e., 22 % of the time, but with the FHP solution subject to an ECOVAT market share of  $\pm 3$  SD, this would only occur with a probability of  $1 - 0.88 = 0.12$ , i.e., only 12 % of the time, essentially halving the risk of curtailment.

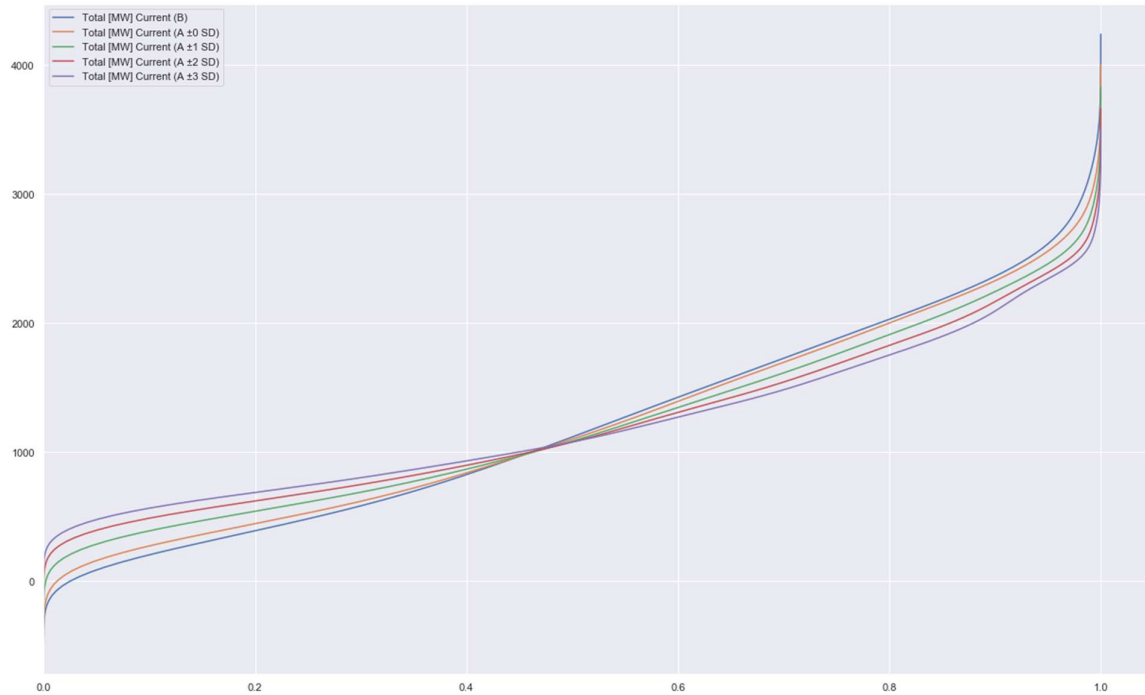


**Figure 63 Belgium: Total [MW] Current CDF (Before, After  $\pm$  SD)**

Taken together, the FHP solution makes it possible to increase the connection of intermittent RES-E by a corresponding percentage, and increase local consumption to the same degree, without being any worse off than before.

Although the evaluation restricts the ECOVAT solution to act on the intraday market, there is in principle nothing preventing the ECOVAT solution from acting on the day-ahead market. However, the intraday market is expected to be economically more advantageous and hence a better focus for the early commercialisation of the ECOVAT solution. Analogously, there is in principle nothing preventing the building heatpump solution from acting on the intraday market. However, the current heterogeneous distribution of building heat pump systems makes broad integration costly, while the NODA solution of indirect control by means of a temperature offset provides an economically feasible solution for acting on the day-ahead market. The division of labour is expected to change as the ECOVAT solution and future grid flexible heat pumps gain market shares, with the future grid flexible heat pumps supporting industry-wide open standards for authentication, secure communication, remote control subject to constraints under local control, and a greater range of internal sensors.

## 6 Conclusion and next steps

The two pilots have demonstrated how P2H flexibility that leverage thermal storage can be used to avoid curtailment of intermittent RES-E or, what amounts to the same thing, increase the effective capacity of the electrical grid. One pilot site (Uden, the Netherlands) was using a large (seasonal) thermal storage facility (the Ecovat) which represents a huge source of flexibility, both in storage capacity as well as in the fact that control actions do not directly impact (or jeopardise) end-user comfort. The second pilot site (Karlshamn, Sweden) was using distributed flexibility provided by a cluster of heat pumps that are used for space heating (and DHW consumption).

The key goal – and challenge – of the pilot validation was to propose – and assess the possibility and barriers of – retrofit solutions using the available P2H infrastructure (incl. off-the-shelf heat pumps that are installed), without introducing additional infrastructure that might be perceived as being too intrusive. Specifically, we wanted to evaluate the creation of dynamic thermal models purely based on measurement data (hence no model creation by a human expert), and the provision of curtailment mitigation services with legacy off-the-shelf heat pumps that are indirectly controlled using an outdoor sensor override control paradigm.

The main learnings are summarized below:

- The kind of services that can be delivered with heat pumps is very much determined by how deterministically it responds to control signals. This in turn is determined by 1) its intrinsic flexibility i.e. its internal controller (as was concluded in WP2, the intrinsic flexibility of heat pumps differs very much among different brands and models) and 2) the accurateness of the heatpump signature model<sup>14</sup> in case of an indirect control strategy (e.g. through an outdoor temperature sensor override).
  - The legacy off-the-shelf heat pumps that were available in the Swedish pilot buildings scored very low on the intrinsic flexibility, and the heatpump signature model that was created by using a large amount of historical data, had limited accuracy (main contributing factors: coarse time granularity, and mixed cycles for space heating and DHW generation). As a result of this, it would be impossible to offer flex services that requires a high level of determinism (like a balancing service), yet a (day-ahead) curtailment mitigation services is still judged to be possible.
  - The heat pumps that were installed early on in the Ecovat, before we had all the WP2 results and insights, scored a bit better on the intrinsic flexibility (at least for the ramping-up cycles ... ramping down proved to be less predictable). Besides, a more accurate heatpump signature model

---

<sup>14</sup> The heatpump signature model is needed to calculate the heatpump control signal profile for a given target consumption profile.

was created based on finer granular measurement data which was collected from specific heatpump characterization tests (gradually improving, and with close collaboration of the heatpump manufacturer). This definitely resulted in a more predictable control signal response that for the Swedish buildings, yet probably still not good enough to provide something like a balancing service that requires a more deterministic response with respect to heatpump consumption (i.e. modulation level, compressor speed) on a 15' time resolution.

- From the WP2 experiments, it has been observed that far better results are achievable with a properly selected heatpump (intrinsic flexibility) and accompanying heatpump signature model. Depending on what level of accuracy is expected for flex delivered by (clusters of) heat pumps, it may even be possible to offer for instance balancing services. Further work will be done in future research - as well as exploitation - projects, to elaborate and improve the heatpump characterization tests to determine their intrinsic flexibility (i.e. fitness-for-purpose) as well as to improve the accurateness of the corresponding heatpump signature model. This clearly will require close collaboration with selected and interested heatpump manufacturers.
- Although (from WP2) it seems to be conceivable to offer valuable services using the indirect control paradigm – which is the only possible solution for off-the-shelf heat pumps in a retrofit context - it is clear that far better results are possible applying the proposed direct control strategy (Grid Flex Heatpump). Further engagement with heatpump manufacturers to increase their awareness of the possible business value, and addressing their concerns, will be a major follow-up action.
- The human expert free building thermal modelling, where the models were created by solely using – limited- measurement data, proved to be successful. Even though the resulting models were created from limited ('flat') training data (due to the fact that the training data was generated from a standard control situation i.e. no specific perturbations to create richer data, and with a thermostat that intrinsically enforces 'flat' data), the models proved to be able to predict the temperature evolution in response to heatpump electricity consumption well. Especially if it was possible between heatpump cycles for space heating versus heatpump cycles for DHW generation. The model did not capture some of the fast dynamics (indoor temperature swings) that were observed, but these were likely due to unmonitored and uncontrollable internal gains i.e. are not related to the chosen building thermal modelling approach. Limiting factors in the pilot tests were:
  - lacking measurements on heat flows i.e. only central heat generation by the heatpump was measured (or estimated); but no information on heat distribution to the multiple zones. The average\_temperature approach that was used was working reasonably well, but ideas resulting from expert discussions in the project on how to apply advanced machine-



- learning approach to estimate heat distribution based on measurements that are available, will be elaborated and evaluated in follow-up projects.
- Lacking information on thermostat setpoints and setpoint changes. In the project, we came up with a methodology to estimate thermostat setpoints based on the collected measurements. While it is envisaged that this can be further improved, it is likely that in near future this issue will be resolved by the widespread availability of IoT thermostats whose setpoints can be accessed remotely.
  - The overall goal of the project was not just provide P2H flex to mitigate RES curtailment, but to do so taking local grid constraints into account. The proposed Flex Trading approach that was implemented through the DCM-centric multi-agent system, is believed to be a key enabling factor. In a more traditional Demand Response scheme, incentive or control signals are sent that may be effectuated for instance through a SG Ready flex interface to the heatpump. It is impossible to predict though if or how many heat pumps will act on the flex activation request, and in which manner, and when precisely. I.e. it might be that they all act in a manner that causes a too high consumption peak, or that none acts because no flex can be delivered without violating a comfort constraint. The proposed FHP solution, with its bottom-up identification and aggregation of both plan and flexibility, and the optimal flex activation decision and disaggregation, addresses this problem (assuming the deterministic response of heat pumps to a control signal is improved: either through better indirect control or through direct control in future: see above). It is known upfront whether or not a problem can be solved through a flex activation, or whether other measures are required. And it can be ensured that an optimal – but especially a grid secure – flex activation is done. Besides, this bottom-up Flex Trading approach is completely in line with the subsidiary principle in support of a more efficient and effective distributed management of the future energy system.

Besides the experimental validation described above, we as well proposed and calculated an impact assessment KPI with respect to leveraging the active control of P2H conversions to mitigate RES-E curtailment. Although the proposed methodology allows for a high-level and statistical analysis, it is believed that the simulation based neighbourhood impact analysis methodology and tool that was developed in T4.2 allows for a more precise and usable analysis that can guide local developments e.g. related to Local/Citizen Energy Communities of district level renovations.



## 7 References

- [1] M. F. Dominguez, E. P. Rivero, C. Caerts and J. Brage, "D1.1 Business case analysis and business model development," *Flexible Heat and Power (FHP)*, pp. 65-69, 2017.
- [2] J. Brage, M. Steen , W. Mazairac, J. Verhaagen, F. De Ridder , G. Suryanarayana, R. d'Hulst, D. Geysen and C. Caerts, "D4.1 Pilot definition," *Flexible Heat and Power (FHP)*, pp. 54-61, 2018.
- [3] M. Lindahl, T. Walfridson, O. Raftegard, J. Benson, M. Borgqvist, E. Lindeblom, B. Tellado, M. Fernandez, J. Van Bael and D. Ectors, "D2.3 Grid flex heat pump design," *Flexible Heat and Power (FHP)*, 2018.

